

## Emulsion Microscopy and Scanning Technique

### 7.1 Visual Measurements Technicians

Of the greatest importance to a research program are the microscopists, variously called visual measurements technicians, scanners, searchers, etc., who aid the investigator by finding events, tracing out long tracks, and making microscope measurements. Although this varies with the type of work being done, the efficiency with which reliable data can be obtained increases with the number of scanners up to an optimum number of two or three per scientist, depending on the project. A larger number of scanners usually puts too great a load on the scientist because he must interpret the ambiguous events. Also some of the scanners usually are in the process of training, and, in addition, the scientist probably will have other matters demanding his attention.

For certain kinds of work the scanner's interpretation of each event should be checked, and the final measurements may often be entrusted only to the most highly qualified person available. For complicated scanning programs, much efficiency will be gained by the utilization of carefully worked out forms for the recording of the data and similar calculation sheets for its reduction.

Among the most useful scanners seem to be people with some scientific training, especially in mathematics; but general intelligence is probably the best qualification. Applicants for positions as scanners in the Lawrence Radiation Laboratory are asked to carry out elementary measurements with the microscope—angles between tracks, horizontal and vertical distances, counting operations—and are also sometimes asked to draw what they see in a field of view of the microscope. The accuracy of the measurements, and the judgement displayed in choosing methods of measurement reveal rather well the potential usefulness of the individual being tested.

The condition of the scanner's eyes is of course a consideration, but it is not as important as might be imagined.

The research binocular microscope has individual eye adjustments so



that differential myopia or hypermetropia are of little importance. Very few people have eyes so poor as to disqualify them as scanners. Most trouble with eyes, when it develops, is found to be caused by faulty microscope adjustment. The alignment of light source, diaphragms, condenser, and objective must be good. The intensity and color of the light should be adjusted for maximum comfort and visual acuity. It is very important that each eye in a binocular microscope see the same field of view both vertically and horizontally. Occasionally rapid scanning can cause nausea, especially when the microscope adjustments are imperfect.

The good scanner is industrious, accurate, patient, careful, fast, neat, and accurate in record keeping, and makes few errors in calculations. To be a good scanner surely requires motivation. A reasonable amount of competitive spirit among scanners is good. An intellectual environment in which to work, development of an "esprit de corps" in the special group to which the individual belongs, the prestige of finding an important event, a belief in the importance of his work, and confidence in and respect for the scientists guiding the work all probably are important. It has been found in some laboratories that physically handicapped people may make remarkably good scanners. Generally in a scanner an appearance of physical well-being and neatness are correlated with good work.

Poor morale and reduced production by scanners are inevitable if the scientists fail to show appreciation and enthusiasm for good work, and willingness to sacrifice personal convenience to the requirements of the research.

The training of scanners should be partially formal, and lectures and reading on the following topics are recommended: the microscope, especially practical details of its alignment and use; mathematics, especially statistical treatment of data, confidence intervals, and elimination of bias; the emulsion instrument, exposure and processing procedures; elementary particle physics; the elements of particle classification and behavior in emulsion; microscopic measurements, measurements of ranges, space angles, volume densities, flux densities, scattering, and gap measurements.

While working the microscopist preferably should be seated facing a dimly lighted wall. Moving objects and bright spots at the edge of the field of vision are distracting and cause eyestrain because the eye is drawn to them.

Music during work has been found good, especially if local control of loudness can be exercised, and if the type of music is chosen well. FM radio tuned to "music" stations has been found satisfactory.



Rest periods such as coffee breaks are necessary for relaxation, but have been known to get out of hand when no scientist is working closely with the scanners. It is the general experience of scanners that fatigue affects their efficiency and the morning hours are the best for production. More is accomplished and fewer errors made in the first half day than in the second. If plenty of equipment is available, and the additional inefficiency in training can be tolerated, half-time workers are for this reason sometimes at least as satisfactory as those who work all day.

## 7.2 The Microscope and Its Accessories

The indispensable instrument for analyzing the behavior of tracks in emulsion is a good microscope. Special microscopic accessories and automatic equipment we reserve for other sections. In this we discuss standard scanning equipment.

A most important component of a compound microscope is the object lens or objective. It forms a real image of the object. In the image plane is placed the reticle, so that the real image formed by the objective has superimposed on it any scales and field dividing lines engraved on the reticle. The eyepiece or ocular serves as a magnifying glass to examine the real image formed by the objective.

Objectives are classed either as "dry" or "immersion" lenses. Dry lenses of low power can be used directly for examining the object, but a dry lens of more than about  $20\times$  magnification generally yields a poor image unless used with a cover glass of a thickness for which it has been designed. Dry objectives of high power can be used without a cover glass by shortening the tube length of the microscope or by using a lens with a correction collar which controls the spherical aberration produced by the absence of a cover glass.

Achromatic objective lenses are made using combinations of positive and negative lenses with different refractive indices and dispersions to give the same focal length for two wavelengths of light, and no spherical aberration for one color. Apochromatic lenses, by the use of many lens components, provide for the chromatic compensation of three wavelengths, no spherical aberration for two wavelengths, and little residual chromatic difference of magnification. Semi-apochromatic objectives, usually designated as fluorites (Fl.), provide the same degree of spherical aberration correction as the apochromats, but chromatic compensation for only two colors.

Curvature of the field, which is quite objectionable for photomicro-



graphy and when dip-angle measurements are to be made, can be kept within narrow limits by selecting from the designs that provide other compensations the one that gives the widest angular interval of flat field. The quality of the image that can be produced at high magnification is significantly improved by an immersion lens. Fortunately for nuclear-track emulsion work, a "homogeneous immersion" optical system can be employed.

The first element of the objective is a spherical section, the bottom being flattened. It dips into oil that is placed directly on the emulsion. The refractive indices of the glass, oil, and gelatin are each very close to 1.52. The tracks being viewed are in a medium that is optically homogeneous, and a condition of "homogeneous immersion" exists. Such an arrangement has the desirable features of "aplanic" refraction, freedom from spherical aberration. With it, the highest possible optical resolution can be attained. The resolution is determined by the numerical aperture (N. A.) of the system. The minimum separation that can be detected between two bright lines is about  $(1/2)\lambda/N.A.$ , where  $\lambda$  is the light wavelength in air. The numerical aperture is  $n \sin \alpha$ ,  $n$  being the index of refraction and  $\alpha$  the angle of the extreme ray to the axis. The maximum N. A. provided by a good objective ordinarily is 1.3-1.4, although somewhat higher numerical apertures can be obtained with monochromatic lenses. There does not seem to be any strong reason why emulsion work should not be done with monochromatically corrected lenses.

Carl Zeiss, E. Leitz, and R. and J. Beck make "apertometers" for measuring the numerical apertures of objectives. A test plate, consisting of lines ruled through a thin coating of silver deposited on a glass wedge, is used for observing the spherical and chromatic aberrations in objectives.

Dry lenses do not have numerical apertures exceeding about 0.95, but they are convenient for scanning rapidly at low magnifications. The spherical aberration of the image varies with the depth in emulsion, however, and is a fundamental fault which restricts the use of high-power air objectives in emulsion work. The need for a cover glass with most high-power air objectives is a nuisance, and in any case the image is never good at all depths when the N. A. exceeds about 0.5. On varying the tube length, the spherical aberration at any particular depth can be reduced. Leitz and Koritska make dry objectives specifically for emulsion work, and metallurgical objectives are calculated for use without a cover glass. The image quality, however, suffers in comparison with that of an immersion lens even when objectives of low power ( $20\times$ ) are compared.

The working distance of an objective is important for thick emulsion



microscopy. This is the distance from the object to the lower extremity of the objective. At present there are no commercially obtainable objectives of N. A. more than about 1.32 that have a sufficiently large working distance to scan processed 600  $\mu$  emulsion, the actual thickness of which varies, but may often exceed 300  $\mu$ .

TABLE 7.2.1  
SOME OBJECTIVES SUITABLE FOR EMULSION MICROSCOPY

---

Dry objectives for low power scanning:

1. B and L, Zeiss or Leitz 10  $\times$  /0.25
2. B and L 21  $\times$  /0.50

Dry objectives for scanning thin emulsions:

3. Koristka 26  $\times$  /0.65
4. Cooke (M1422) 40  $\times$  /0.85
5. Leitz Ks 47  $\times$  /0.65
6. Reichert 95  $\times$  /0.75

Oil immersion objectives for scanning thin emulsions only:

7. B and L Apo 61  $\times$  /1.40/280  $\mu$
8. Cooke Apo 80  $\times$  /1.32/280  $\mu$
9. Leitz Apo 90  $\times$  /1.32/280  $\mu$

Oil immersion for emulsions up to and around 600  $\mu$ :

10. Leitz 22  $\times$  /0.65/500
11. B and L Fl. 40  $\times$  /1.00/400
12. Leitz Fl. 70  $\times$  /1.30/350
13. B and L 98  $\times$  /1.30/300
14. Cooke Fl. 45  $\times$  /0.95/400
15. Leitz Ks Apo 100  $\times$  /1.32/370
16. Leitz PLANO Apo 100  $\times$  /1.32/420
17. Koristka Fl. 100  $\times$  /1.25/530

Oil immersion objectives suitable for thick emulsions:

18. Leitz Ks Fl. 53  $\times$  /0.95/1000
  19. Koristka 55  $\times$  /1.00/700
  20. Koristka Apo 65  $\times$  /1.20/600
  21. Koristka 30  $\times$  /1.10/1000
  22. Koristka 30  $\times$  /1.00/3000
  23. Cooke 25  $\times$  /0.65/2000
  24. Cooke 45  $\times$  /0.85/1500
  25. Leitz Ks 22  $\times$  /0.65/2200
  26. Koristka 55  $\times$  /0.90/1350
  27. B and L Fl. 40  $\times$  /1.00/1500 (on special order)
  28. Leitz L591 100  $\times$  /1.32/700 (on special order)
  29. Zeiss HI 50  $\times$  /1.00/1900 (normally takes 240 mm tube)
  30. Zeis Monochromatic HI 50  $\times$  /1.35/600 (on special order)
-



Hodges\* (H 60) has gathered data on many lenses suitable for emulsion microscopy. Table 7.2.1 was prepared with his help. Lenses representing both quality and thrift are tabulated. Some manufacturers are not listed simply because our experience at the Lawrence Radiation Laboratory is not sufficiently broad to know all the available products.

An exceedingly large working distance combined with a good numerical aperture is needed for some special emulsions of great thickness (Y 57), and for viewing events in the emulsion from the glass side of the plate. In a certain method of track tracing one also must be able to examine tracks in the lower of two plates that are superimposed. For such tasks the  $30 \times /1.00/3000 \mu$  objective of Koritska deserves especially to be known. One of several types of reflection objective may in the future be found adequate for these purposes, but commercial lenses of this type now known to be available are not of sufficiently high quality for emulsion microscopy.

Objectives have either a bayonet mount, which is accurately alignable, or a turret mount containing three to six objectives. While the turret mount is the more convenient, a mechanically excellent turret and objective mount are needed. Each lens in turn should be rotatable with axis well aligned to the same position. A satisfactory tolerance is about 0.001 inch. It is convenient if the lens and mount are designed so that each lens is focused at the same depth. Such an arrangement is *parfocal*. It avoids mechanical interference between plate and lens on rotating the turret.

When altering a microscope for a special purpose, one must remember that objective lenses are designed to provide a corrected image only at a standard tube length, which is 160 mm (Leitz and Koritska use 170 mm). This length is measured from objective-shoulder to eye-tube extremity, but allowance for the effect of any auxillary lenses in the light path must be made. Some microscopes provide additional magnification in the binocular body.

For viewing tracks in emulsion light is transmitted through the glass plate on which the emulsion is mounted, as well as through the emulsion itself. To obtain the maximum resolving power the light should reach the track grains as a highly convergent beam, and then diverge so as to fill uniformly the aperture of the objective. To realize the full numerical aperture of the objective, a lens, the substage condenser, with a numerical aperture comparable to that of the objective should be used to form the beam. It also must use oil immersion if a

\* Many facts regarding equipment for microscopy were obtained from Mr. J. C. Hodges, and the points of view presented here on this subject have been strongly influenced by Mr. Hodges' thinking and experience.



numerical aperture exceeding unity is ever to be achieved. In nuclear-track work this is usually inconvenient, but may be tried when a particularly difficult problem of optical resolution is encountered.

The theory of optimum resolution in a microscope is complex because of subtle scattering and interference effects, and it is not always true that the highest resolution is obtained with the N. A. of the condenser equal to that of the objective. The finer detail of the image in emulsion is sometimes best apprehended with condenser apertures substantially less than that of the objective. One possible explanation is that the scattering of light in the emulsion in effect increases the condenser aperture (H 60).

Because the emulsion sheet is usually attached to a glass plate about 1/16 inch thick, a minimum working distance of about 2 mm is required of the substage condenser. This is seldom attained in condensers of N. A. in excess of 1.3. For most scanning the simple and thrifty two-lens Abbe condenser of N. A. 1.25 is recommended.

The mounting of the condenser is sometimes inadequately engineered. It should have a sturdy mount with means to accurately center the condenser on the axis of the objective and to align their axes. The diaphragm and height adjustments should be easily accessible, but the alignment adjustments, once made, should be clamped.

The condenser height should be adjustable by means of a smoothly sliding rack-and-pinion mechanism. The condenser should move accurately along its common axis with the objective. An externally located iris diaphragm to control the aperture, and as a means for aligning the substage optics, is an essential part of the condenser. It should be possible to reach the control arm easily. The iris must close to a small well-centered opening. In normal use the iris is opened just enough to accept the bundle of rays that fills the full aperture of the condenser-objective combination. A larger opening causes loss of contrast by light scattering in the emulsion.

It is now believed that the image in the microscope of an object by transmitted light is formed in the main just as the image of a self-luminous object is imaged. This is in contradistinction to an old theory of Abbe.

In dark-field illumination, the condenser is constructed so that the field is traversed by light at an angle too large to be accepted by the objective. Then discontinuities in the field scatter light, and the track grains appear as bright points. Extensive employment of dark-field illumination seems not to have been made in nuclear-track microscopy. One reason is that the adjustments to maintain the dark field vary with the depth in the emulsion.

Dark-field illumination with the light coming from above appears to



offer interesting prospects for viewing very fine-grain emulsions. The mere presence of a grain is detectable, even if it is too small to be seen by transmitted light. Use of such equipment for this purpose has been described by Rechemann (R 55.1).

An eyepiece lens is used to magnify the real image produced by the objective. In order to maintain the off-axis image quality, even the simplest oculars generally consist of a pair of lenses, a field lens, and an eye lens; the field lens being the more remote from the eye and having, in the Huygenian form, a larger focal length than the eye lens, and in the Ramsden form, an equal focal length. As generally constructed, the real image produced in the Huygenian eyepiece lies between the eye lens and the field lens. The distortion of the image is somewhat greater than in a Ramsden eyepiece. For nuclear-track microscopy, the larger amount of chromatic aberration of the Ramsden type of ocular is not an important defect. The best theoretical separation between the lenses in a Ramsden eyepiece is their common focal length, but this brings the exit pupil too close to the eye lens, and also brings into focus dust, scratches, and other imperfections of the surface of the field lens. The lenses are, therefore, usually separated by only two-thirds of their common focal length, and the field lens falls between the eye lens and the focal plane in which is mounted the reticle.

The two-element Huygenian negative ocular and simple Ramsden eyepiece have now been largely superseded by more complex structures, but they illustrate the two basic types. Trade names for more highly corrected lenses include such lenses as the Hyperplane, Kellner Complanatic, Planascopic, Periplan, and Holoscopic. The most highly developed lens types are the compensating eyepieces which are carefully computed to correct apochromatic objective defects.

In the Holoscopic eyepiece the eye lens-to-field lens distance can be varied and the spherical aberration of various objectives eliminated. The magnification changes with the change in distance. Since no objective is corrected fully, the eyepiece may be selected to have built-in aberration to compensate as much as possible for those left in the objective. It is often recommended that compensating eyepieces be used with objectives of N. A. greater than 0.65, with all apochromats and with all plano-objectives. On the other hand, they should not be used with objectives requiring no chromatic compensation, such as achromats of N. A. less than 0.65, because the chief compensation is for a chromatic difference of magnification.

We do not make a broad recommendation for the use of compensating lenses in emulsion microscopy because many other features besides perfect achromatism—especially when the microscope is used almost



monochromatically—are more important. For example, the field generally is more curved when compensating eyepieces are used.

Bausch and Lomb (B and L) make an Ampliplan projection eyepiece which flattens the field and which is useful in photomicrography. Carl Zeiss makes the Homal eyepieces for a similar purpose. The Hyperplane eyepiece of Bausch and Lomb is made for use with achromatic objectives for flattening the visual field. Leitz Periplan eyepieces help produce flattened fields with a minimum of peripheral distortion. The American Optical Company manufactures the Planoscopic eyepiece for use with achromatic objectives to flatten the field. Another intermediate compensation ocular is the positive Orthoscopic lens of Zeiss and Beck.

Coated lenses that reduce reflections help to maintain the image contrast.

Wider fields offer considerable advantages for nuclear-track microscopy, but the field width is limited by the inside diameter of the binocular eye tube, which is 23.3 mm. Development of binocular microscopes with larger tubes probably should be encouraged. B and L  $10\times$  and  $15\times$  wide-field lenses are satisfactory, and the Leitz GF series of oculars is especially good for wide-field viewing. Sometimes the advantage of a wide field for track tracing is so great that it is best to widen the field of imperfectly corrected lenses by removing aperture stops, even if the image quality near the edge of the field becomes poor. To obtain a wide field of view, positive oculars (Ramsden type) are most extensively used. The Kellner eyepiece chromatically corrects the eye lens and at the same time increases its focal length so that it has a high eye point. Such an eyepiece may be constructed with an achromatic doublet for an eye lens and the plane side of the lower lens away from the eye lens.

The eyepieces should fit snugly into the eye tubes. Loose eyepieces may skew their axes with respect to each other.

Table 7.2.2 lists some oculars for emulsion microscopy.

TABLE 7.2.2  
OCULARS FOR EMULSION MICROSCOPY

- |    |  |
|----|--|
| a. | $5\times$ Hyperplane (B and L)                               |
| b. | $6\times$ Periplan (Leitz)                                   |
| c. | $10\times$ , $15\times$ Wide field (B and L)                 |
| d. | $10\times$ , $15\times$ Kellner (Cooke)                      |
| e. | GF $10\times$ , $16\times$ , $20\times$ , $25\times$ (Leitz) |
| f. | $10\times$ , $16\times$ Periplan high eye point (Leitz)      |

This does not by any means exhaust the list of satisfactory lenses, but perhaps may be a guide for choices in lenses.



Almost any ocular listed will be fairly satisfactory with the objectives given in Table 7.2.1, but for critical work particular combinations are best. For example, a combination of the Leitz PLANO and the  $10\times$  GF is good for providing a flat field. Kellner oculars give maximum reticle coplanarity for precise range measurements, while the GF series are good in combination with high N. A. objectives for grain counting and other requirements of good seeing, magnification, and wide field. The lower powers listed as *a*, *b*, and *c* are suggested for preliminary scanning work. High eye point lenses are convenient when, for data recording etc., a microscopist wishes to wear spectacles while scanning.

Not listed but good for work with apochromatic objectives of high power are such compensating eyepieces as the Zeiss (Jena) K20 and K30 of very high magnification, and the B and L  $15\times$  and  $25\times$ . These are used in the Lawrence Radiation Laboratory for measurement work at high powers. They are positive lenses. This simplifies the incorporation of a reticle into the focal plane.

Measurements in the field of a microscope are best made with the aid of a good reticle (also reticule and graticule in Britain). This usually takes the form of a thin disk of glass mounted in the focal plane of the eyepiece. By means of lines ruled on the glass the field may contain crossed lines and be divided into smaller areas. It may also contain a scale of length. The reticle is placed differently in the eyepiece depending on whether it is a Huygenian or a Ramsden ocular.

Suppose a track is seen in focus with a Huygens eyepiece. This means that within the ocular, behind the first or field lens, a real image is formed. On the other hand, the real image that is seen exists, not between the eyepiece lenses, but in front of the field lens in a Ramsden eyepiece. If a scale is to be used to measure distances in the real image, it must be placed at the point where the real image is formed. The position of the image varies somewhat with the eye of the observer. It is more convenient for the placement and adjustment of the reticle to use a Ramsden eyepiece. Such eyepieces usually will be provided with an adjustable mounting ring for the reticle. Commercial reticles both ruled on glass and photographically reproduced are available in a number of forms. They are rather expensive, however, and usually it is inconvenient to obtain a ruling of the desired excellence. For these reasons reticles of fine quality are manufactured in the Lawrence Radiation Laboratory shops to meet various needs. Figure 7.2.1 is a piece of equipment that has been built to rule reticles on glass with a diamond point.

Figure 7.2.2 shows a standard form of reticle used at the Lawrence Radiation Laboratory. They range in complexity from simple crossed.



lines to numerous lines dividing the field into areas, and also include scales for length and angle measurements.

One of each ocular pair in a standard emulsion microscope should be fitted with a reticle. The other probably should contain a similar disk without engraving. The dominant eye of the microscopist should look at the reticle.

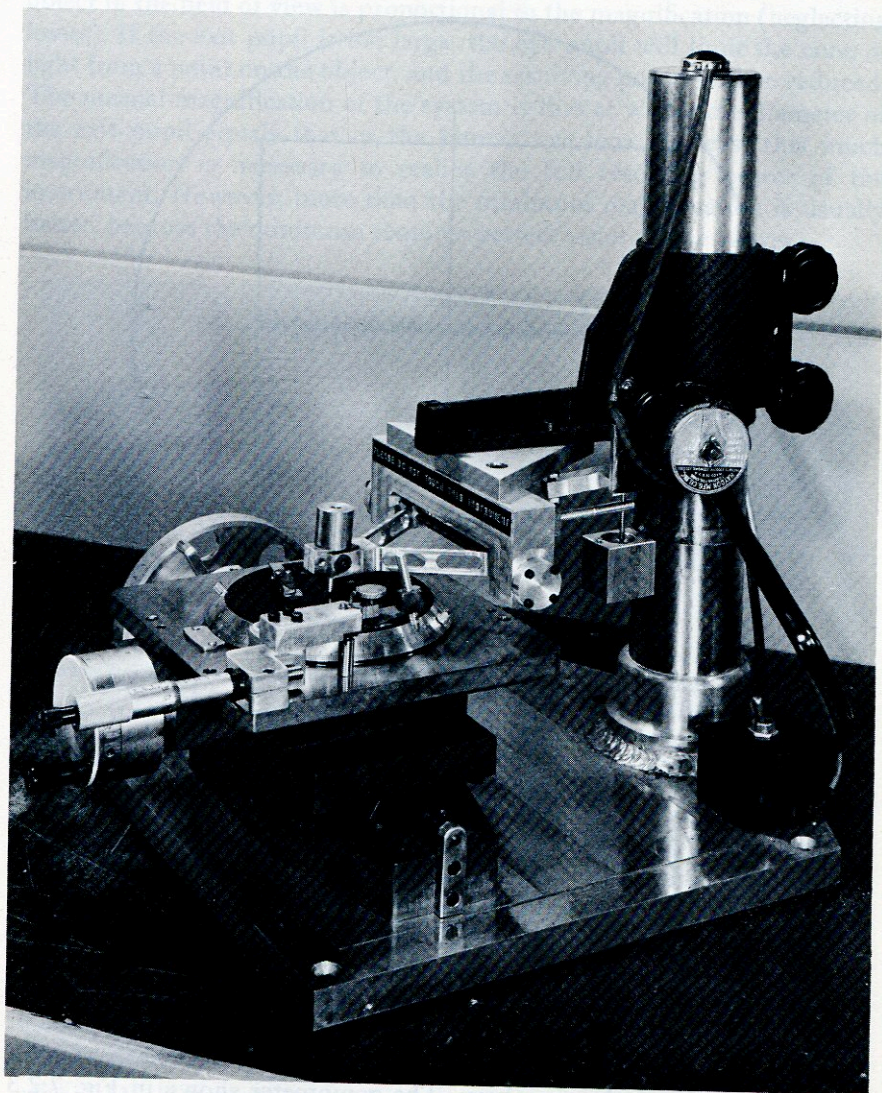


FIG. 7.2.1. Diamond-point ruling machine for making reticles (IDLRL).



In ruling lines on glass, a very fine line, but at the same time one that is clearly visible when one's attention is directed to it, should be the goal. There are, in addition, other considerations. The divisions must be uniform. The scale length must be limited to the size of the diaphragm stop. For granularity measurements the scale should encompass only the portion of the field over which the image is good. The reticle should be

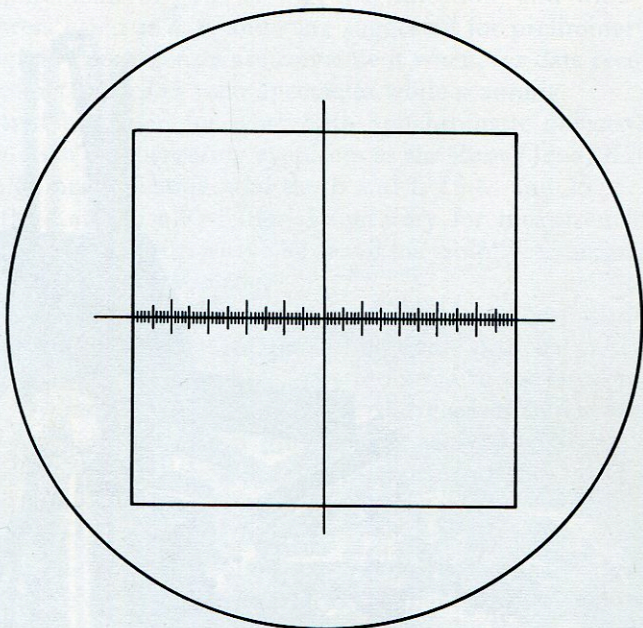


FIG. 7.2.2. Example of a standard pattern ruled on glass for emulsion scanning and measurement (IDLRL).

well centered, so that on rotating an ocular the center does not move. It may be necessary to improve the fit of the ocular in the eye tube for this condition to be achieved. It is easier to obtain accurate centering if the disk is cut to the inside diameter of the ocular using the center of the engraved pattern as the center of rotation.

To make angle measurements with the reticle it is usual to employ a goniometer. The goniometer normally consists of two parts, the rotatable barrel into which the eyepiece containing the reticle is fitted and a second part, the body, which is clamped to the eye tube. These parts fit closely together, and the rotation of the barrel can be measured by a scale and vernier at the periphery. The goniometer shown in Fig. 7.2.3 was developed several years ago at the Lawrence Radiation Laboratory



to meet the special needs of emulsion microscopy. It is described more fully by Hodges (H 60).

A stop which limits the aperture of the optical system of the microscope may be found in the objective. The image of this stop produced above the eyepiece is the *eye point*, or *exit pupil*. When the exit pupil is as large as the eye pupil, the amount of light entering the eye from an object in the field of view is proportional to the magnification (neglecting losses). If the exit pupil is too large, the eye pupil will limit the cone of light from a point on the object, and the resolving power will be reduced. The normal magnification of the system is that at which the diameter of the exit pupil equals that of the human eye lens. At least this much magnification is necessary to realize the full resolving power of the instrument. However, more than the minimum magnification is usually better, because the minimum requires perfect vision in the viewer.

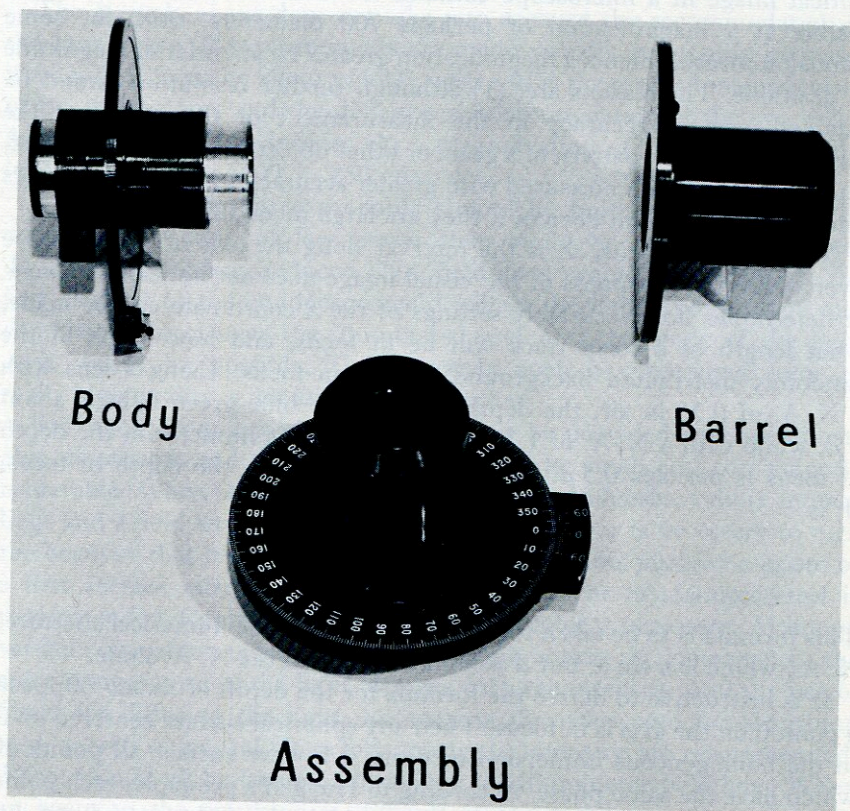


FIG. 7.2.3. Photograph of a standard goniometer made in the Lawrence Radiation Laboratory shops (IDLRL).



If the exit pupil is reduced, a smaller area of the eye lens will be used and the resolving power of the eye lowered.

The eye point distance is sometimes as little as 4 mm. It usually is listed with other lens specifications in the manufacturer's catalog. High eye-point oculars can be obtained for people who wish to wear glasses or who for some other reason cannot bring their eyes close to the oculars.

The minimum separation that two points must have to be resolved by the microscope-observer combination is, of course, affected by the magnification. The magnification must be sufficient so that the angular interval separating the points exceeds a minute of arc, the resolving power of a good human eye. The smallest resolvable separation of two nonluminous points, when this condition has been met, is determined by the diffraction pattern of the light, and cannot be reduced by higher magnification. These considerations lead to the conclusion that the optical image in a microscope contains no more information than that visible at a magnification of perhaps 700 diameters. Still, for some emulsion measurements a magnification greater by an order of magnitude is desirable. The reasons are: (1) although further resolution cannot be attained, greater accuracy in the measurement of the center of the circular diffraction pattern of a grain or other object can thus be achieved, and (2) distances are measured with greater accuracy by filar micrometers and other mechanical devices if they are large in an absolute sense.

The depth of focus,  $\Delta$ , is the interval along the axis of the objective over which the sharpness of the visual image does not noticeably change. It determines how accurately settings of the  $z$  coordinate can be made, what length of a steep track will be in focus, and how much of the randomly distributed background will be in focus. Using a lens with a N. A. of 0.25 in air, the depth of focus for blue-green light is about  $8\ \mu$ , while with a N. A. of 1.25 and homogeneous immersion, the depth of focus is perhaps  $0.5\ \mu$ . The general formula for the depth of focus,  $\Delta$ , is

$$\Delta = \frac{\lambda}{4n \sin^2 \alpha/2}$$

This formula is to be taken together with that for the numerical aperture, N. A., which is  $n \sin \alpha$ , but  $\Delta$  is not a function of the N. A. alone.

It is instructive to derive the formula for the depth of focus. Suppose a point  $O$  on the axis is in focus. Then any spherical surface centered on  $O$  in the homogeneous immersion medium is a wave surface all points of which have the same phase. According to Huygen's principle, each point on any mathematical surface through which the light passes can be considered a new source, and the subsequent behavior of the light is



determined by the phase and intensity distribution over this surface. Lord Rayleigh introduced a further principle, the Rayleigh limit, according to which the focus of a nearby point is altered only imperceptibly if light from it reaches the surface with no relative phase changes exceeding  $\pi/2$ .

For another point,  $O'$ , displaced a small distance  $\epsilon$  along the axis, the maximum path difference is  $\epsilon(1 - \cos \alpha)$ , where  $\alpha$  is the angle of the extreme ray. We set this equal to  $\lambda/4n$  where  $\lambda$  is the wavelength in air, and put  $2\epsilon = \Delta$ , the interval over which the focus will be satisfactory. The above relation is then found for  $\Delta$ . For  $\alpha$  not too large, this formula implies that the depth of focus is inversely proportional to the numerical aperture times the magnification of the objective. The angle  $\alpha$  normally exceeds the angles with the axis made by extreme rays at other points of the light path. It controls the focal depth of the whole instrument under these conditions.

The formula above does not take into account the accommodation of the human eye. If measurements are made visually, it possibly increases the depth of focus by about  $nD/M^2$ , where  $M$  is the over-all magnification of the microscope, and the distance of accommodation of the eye varies from a distance  $D$  to infinity. At a magnification of 1000, for example,  $(nD/M^2) = 0.38 \mu$  if  $D = 250$  mm.

The ideal light source probably should be built integrally with the condenser. A lamp of low power then could be used and the heat dissipation problem reduced. No field lens would be required; the first element of the condenser could collect the light. Independent and complete control over the illuminated area and the angle of the light cone would be possible. Unfortunately such a commercial unit of really high quality is not known to the writer.

For emulsion microscopy the lamp must be provided with an adjustable diaphragm and the light source should be small and conveniently centerable. When not built integrally with the condenser, a more intense light and a field lens are needed. Generally a mirror is necessary to turn the beam so that it is along the optical axis. For this purpose a prism or a first surface mirror of evaporated aluminum or of stainless steel is recommended. Control of light intensity and color is necessary. Although variable transformer control of the light source is convenient, the color-temperature of the light changes with the intensity, and the use of filters for diffusing the light, for varying the color, and for absorbing heat, as well as neutral filters for varying the intensity, are recommended. These should all be located adjacent to the illuminator field lens. When an event in the emulsion is difficult to see and interpret, it is often helpful to vary the light intensity, but if no heat absorber is used, the



emulsion—especially wet, thick emulsion—could be overheated at the focal point and be destroyed.

Although generally a green filter is best for scanning, a blue filter having good cut off for long wavelengths will give better resolution with a well-corrected objective. On the other hand, when events are difficult to see deep in the emulsion because so much light is scattered by intervening tracks and other scattering centers, a red filter may improve the image. Interference filters are sometimes used but they discard much of the light and probably do not have special merit for this work justifying their cost, unless monochromatically corrected optics are used.

Table 7.2.3 is a list of recommended color filters prepared by Hodges.

TABLE 7.2.3  
LIGHT FILTERS FOR EMULSION MICROSCOPY

Type	Solid glass	Gelatin sandwich
Neutral	B and L No. 31-34-67, 20% transmission B and L No. 31-34-68, 10% transmission	
Heat absorbing	Corning Aklo 1-59	
Medium green	Corning 4-65, 4-68	Wratten 54, 58
Deep green	Corning 4-72, 4-74	Wratten 62
Medium blue	Corning 5-59, 5-60	Wratten 2A
Deep blue	Corning 1-64	Wratten 47

Critical illumination puts an image of the bare light source in the plane of the emulsion. With this type of light an achromatic condenser is needed, and the source must be structureless, or its features will be seen in the field of view.

An arrangement known as Köhler illumination is favored. To provide it, diffusing filters are removed and the filament, which should be as small as possible, is focused and centered in the plane of the substage diaphragm. The light beam is made coaxial with the condenser and objective lenses. The image of the light source diaphragm is then focused in the emulsion. Since the source diaphragm is placed just in front of the field lens, this is practically equivalent to putting the image of the field lens in the emulsion.

On putting diffusing filters in the system, the Köhler illumination condition is modified, but improved uniformity of illumination is



obtained. Because of the finite area of light source and the imperfections in the field lens, it is not possible to obtain ideal Köhler illumination in any case.

Convenience for obtaining optical alignment is important. Equally important is the maintainance of this condition once achieved. This should be accomplished by mounting the light bulb, mirror, substage optics, and microscope body rigidly together with accessible screw alignment adjustments for each. The mirror is particularly troublesome unless three-dimensional screw adjustments can be made. To keep the mirror and lenses clean and the surfaces unscratched, the illuminating system should be housed.

At the Lawrence Radiation Laboratory a unit made by the American Optical Company and known as the Ortho-Illuminator is used for microscopy.

Mechanical features of a microscope considered important from the point of view of the nuclear-track plate scanner are the mechanisms that hold the plate and bring about motions of the plate relative to the objective lens. These features must consist of translations along three axes that are mutually perpendicular and, ideally, of rotations about two axes.

As an example of a successful design for a stage of this sort, one can refer to that of Hilding Slätis (S 58.3). (See Fig. 7.2.4.)

The motion parallel to the optic axis (the  $z$  axis) of a microscope normally is brought about by the focusing controls of the microscope. Here one desires a linear translation that is proportional to the angle of rotation of the focusing knob throughout its range of rotation, and this should be calibrated directly in microns. The knob should turn easily and very smoothly, and the engraving on it should be large and clear for easy, accurate reading. Hydraulic coupling of the control knob to the fine focus has been built into a number of special microscopes, and some of these have been very successful. Two fine focusing speeds are desirable.

The substage condenser height usually is changed by a rack and pinion. Since a good microscopist continually adjusts the condenser, the knob controlling the condenser height should be readily accessible.

Binocular vision, although it adds considerable complexity to the microscope, is greatly preferred for prolonged scanning when one has two good eyes. On the other hand, a one-eyed person can also do emulsion scanning quite successfully. Binocular vision with a high power microscope does not imply stereoscopic vision. Owing to the short working distance of a high power objective, the images for both eyes must be derived from a single objective. To retain the full aperture



of the system, this must be accomplished by a partially reflecting and partially transmitting optical element, and means must be provided for varying the interocular distance through its range, for adult men, of 56 to 72 mm. The adjustment also varies the tube length of many microscopes. When it does, it is somewhat undesirable because the magnification is then changed, and because the best image from an objective is obtained at only one particular tube length.

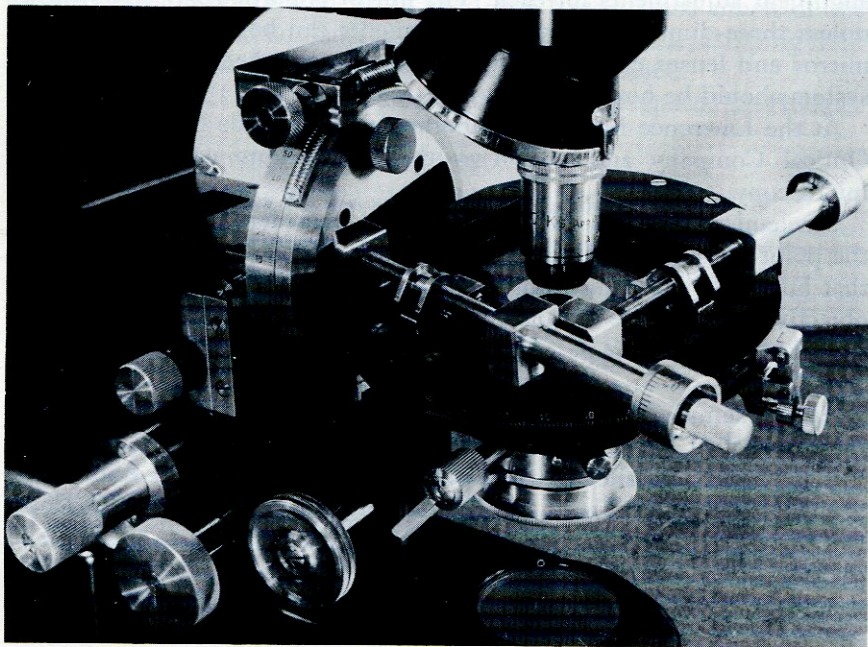


FIG. 7.2.4. Stage at the Nobel Institute providing translation along three perpendicular axes and rotations about two of them. (Courtesy H. Slätis.)

The writer believes that binocular microscopes that furnish oculars with their axes parallel, are preferable. The scanner's eye seeks a field at a distance from the eye that requires least effort for accommodation. This is probably far enough so that parallel eye tubes are most natural, although it is argued that in looking somewhat down ( $45^\circ$  is preferred), as one does in a microscope, that infinity is not the most frequent object distance in one's environment. On first using a binocular microscope, many people fuse the images better with nonparallel eye tubes, but virtually none have permanent difficulty with parallel eye tubes if their eyes are normal, and most come to like parallel vision.



The *parity* of the image may be of importance in some kinds of scanning. In most microscopes left becomes right, and *away* becomes *toward*. This symmetry is not common to all viewing systems, however, and for measurements in which the left-handedness or right-handedness of coordinate axes is important, one must determine whether or not the optical system reverses the parity of the object.

The following are some of the desirable features and accessories of a general purpose nuclear-track scanning microscope that can be provided without excessive cost: (a) objectives as follows:  $100\times$  oil immersion with a working distance of at least  $350\mu$ ,  $45\text{--}55\times$  oil,  $20\text{--}25\times$  oil, or a  $20\times$  dry. A  $10\times$  dry is also desirable. (b) A turret mount, cocentered well enough so that the middle of the field of any of the objectives will be found in the field of the  $100\times$  objective. The lens lengths should be adjusted or collars used so that the lenses are parfocal on rotating the turret. (c) A binocular body with separate focus control of one ocular and sufficient range of interocular distance. Parallel eye tubes are preferred. (d) Standard oculars, perhaps  $10\times$  wide field, but occasional need of  $5\times$  and  $15\times$  to  $25\times$  suggests that these should also be on hand. High eye-point oculars are also sometimes needed. (e) A goniometer for the dominant eye ocular, in which should be mounted a reticle of good quality. (f) Controlled Köhler illumination with color and heat absorbing filters, intensity control, and adequate heat dissipation. The light source diaphragm control should be within easy reach, and there should be alignment adjustments on the light source. The source should be rigidly mounted so as to be integral with the microscope. (g) A condensing lens with an N. A. of at least 1.25, and possibly another of long working distance with an N. A. of about 1.00. It should have a sturdy, well-aligned mount with centering adjustment, diaphragm, and height adjustments within easy reach. (h) A mechanical stage of sufficient area for the largest plate to be scanned and rotated. It should have screw drives for several centimeters in both the  $x$  and  $y$  directions with the screw error no more than 0.1% for all distances greater than 1 mm. The ways of the stage should be smooth enough in one direction to make fairly good multiple scattering measurements possible. A noise level of  $0.2\mu$  over a 1-cm interval of the screw is acceptable. The stage should be mounted so that the  $x$  and  $y$  axes are accurately perpendicular to the  $z$  direction. This direction is defined by the motion of the objective in focusing. Incidentally, it is important that the objective axis be accurately along the line of its motion, and that the condenser be coaxial with it.

One's equipment problems are greatly reduced if he can standardize on certain pellicle sizes. The writer's equipment is designed to accommodate conveniently pellicles and plates of  $1\times 3$ ,  $1\times 6$ ,  $3\times 6$ ,  $6\times 9$ ,



and  $9 \times 12$  inches. Apochromatic objectives are desirable, but the loss in image quality in going to achromats for lower powers and fluorites for higher powers and/or higher apertures is often undetectable in monochromatic use. When necessary in emulsion work savings in equipment costs can be made by using achromatic and semi-apochromatic lenses with small loss in working efficiency. The expense of apochromatic lenses of large aperture is largely wasted unless they are used under the conditions required to obtain the ultimate resolving power.

The quality of microscope lenses manufactured in recent years, especially objectives and condensing lenses, is said to have deteriorated in the features of which an uncritical user would not be aware. The tube length for which the objective gives the best image is often not the standard 160 mm, and nearly all optical companies sell objective and condensing lenses that do not attain as high numerical apertures as claimed. In the purchase of such equipment the buyer will serve all microscope users if he demands that the lenses be as specified.

Figure 7.2.5 shows a standard desk and microscope arrangement developed largely by H. H. Heckman and James Hodges.

The  $11 \times 20$  inch mounting surface on the stage enables one to scan the whole area of a large plate. When using the model shown, one depends on a grid to locate events in the emulsion. The plate is translated and rotated on the stage as desired. It is held down by wads of Plasticum, a modeling clay obtainable in art stores.

Variations of the mounting surface are in use that provide clamps for plates of specific sizes. A standard mounting surface also has been developed in which has been jig-bored a set of very accurately located holes. Steel strips similarly drilled are cemented to the plates of any standard size and, by means of hardened steel pins dropped through holes in the strips, the plate can be located in positions reproducible to 2 or 3  $\mu$ , and any portion of the plate can be scanned. Translation of the stage perpendicular to the optic axis is effected by precision screws. The stage is not level but is tilted at  $12^\circ$  to the horizontal. The stage travel is 120 mm in each direction. The counter shown to the right enables one to read off the  $x$  coordinate to 1  $\mu$ , and the  $y$  coordinate is read out to the nearest micron by means of a micrometer dial and vernier. On some microscopes all three coordinate axes are fitted with direct reading counters which are superior to scales. In the  $z$  coordinate measurement one also may introduce the shrinkage factor by an appropriate mechanism so that original vertical coordinates of points are read off directly. A goniometer eyepiece reading to tenths of degrees by means of a vernier is shown. A light source with an integral first-surface mirror, a variety of filters, and an adjustable diaphragm is



mounted on a common base with the microscope. A good optical line-up once obtained can be retained indefinitely. The larger bottle in the photograph contains alcohol, and the small polyethylene bottle supported in an inverted position holds immersion oil. When kept in this way, the oil remains free of troublesome bubbles. On the pad is a

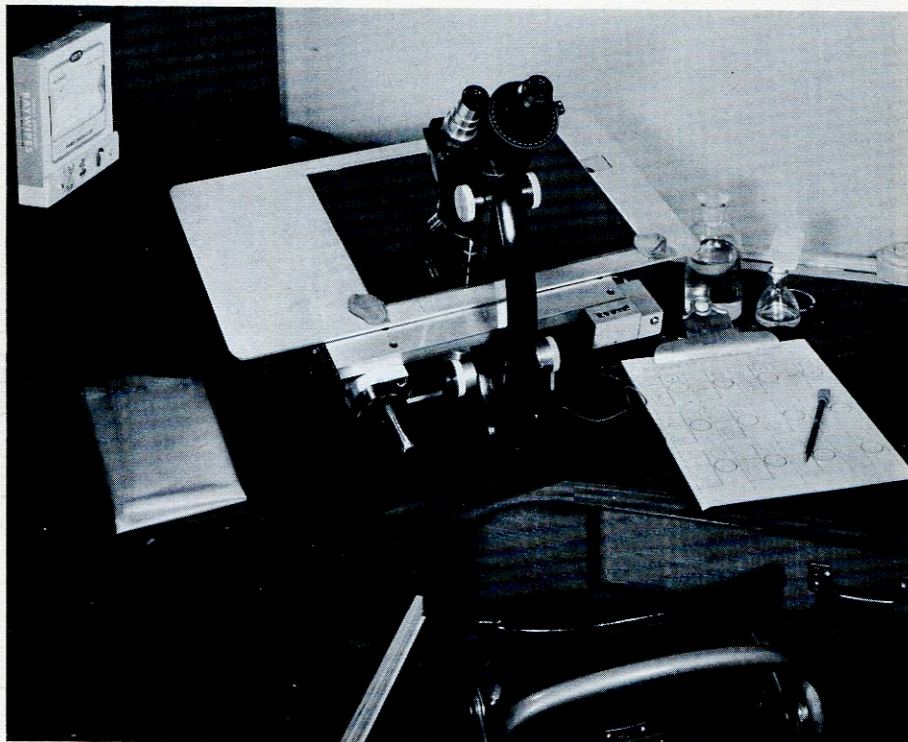


FIG. 7.2.5. Standard scanning equipment in the Lawrence Radiation Laboratory. The surface on which the plate is mounted is interchangeable depending on the plate size and whether or not the plate is provided with alignment strips (Section 4.4) (IDLRL).

printed form developed for recording range measurement data. The folded plastic sheet is a dust cover for the microscope. The tissue paper is used to wipe oil off metal, glass, and emulsion surfaces and for general cleanliness. The drawer contains extra oculars and objectives as well as writing supplies. The chair is of a type designed for stenographers which gives support in the small of the back when properly adjusted. The height of the chair and the tilt of the microscope tubes (about  $45^\circ$  from the vertical) are adjusted so that the scanner sits in an upright, unstrained position with his body close to the microscope.



distance. When difficulty is encountered, the field of view should be examined by each eye in turn. The focus of identifiable grains should be compared, and objects near the boundary of the field of view should be examined to determine whether their appearance and position are identical for each eye. Sometimes the axes of the oculars may be skew lines rather than parallel (or in some microscopes intersecting) lines.

If the axes are skewed it will certainly bother the scanner. Very rapid scanning and focusing also can cause eyestrain from the rapid and continuous eye movements required. On the other hand, a limited amount of this kind of work is an excellent eye exercise and may improve the eye muscle tone.

Scanners wearing correcting glasses may often discard their glasses for scanning if the correction is merely for myopia or hypermetropia. If much astigmatism or heterophoria is present it is best to wear the glasses. Special high eye-point oculars may then be required to avoid damaging the spectacles by pushing them against the oculars.

An eyepiece goniometer should be mounted so that when it reads  $0^\circ$ , one of the diameter lines of the field is aligned with the  $x$  axis. This may be tested by setting the goniometer to zero and translating the stage along the  $x$  axis. A point in the field on the diametral line should then follow it accurately for its entire length.

Bubbles in the oil cause a poor image to be formed. Bubbles can be seen if an ocular is removed and one looks down the eye tube. Any bubbles under the objective lens will then be visible. Use a fine wire or the edge of a piece of paper to remove the bubbles while watching them down the eye tube. Do not use oil of too high viscosity, because bubbles once formed come out very slowly. Do not permit air to be sucked or blown through the oil. Bringing certain types of objectives down on top of oil traps air and the oil for such objectives should always be introduced by capillary action.

In choosing the viscosity of an immersion oil, one must keep the index of refraction close to 1.51 while at the same time compromising two incompatible requirements. In order that bubbles produced in the oil be quickly eliminated, the viscosity must be low. In order that the oil remain between a long-working distance objective lens and the emulsion, especially when the stage is tilted, the oil viscosity must be high. While cedar oil was formerly much used for microscopy it has now largely been displaced for nuclear-track work by oil which does not dry out and harden.

One of the earliest steps in the training of a microscopist is the exercise of care in lowering an oil-immersion objective by means of the



coarse  $z$  motion on to the emulsion. It is recommended that this be done with the plate dry. One carefully watches the gap between objective and emulsion from a position to one side while the objective is lowered. When it is a few tenths of a millimeter from the surface, oil is placed on the side of the objective or on the emulsion adjacent to the objective so that it will run down and be drawn under the lens by capillarity. When the lens is within its working distance from the surface, one will be able to see the emulsion through the microscope, and the subsequent  $z$ -coordinate adjustment is best done with the fine-focus control knob.

The motion of the stage and the fine focus should be smoothly controlled by knobs which are reached without moving the body and with the arms in a normal relaxed position supported by the desk. The elevation of the chair and oculars and the tilt of the oculars should be adjusted so no fatigue develops in the neck or shoulders upon prolonged scanning. Eye spacing should be memorized so that this can be the first adjustment checked on the microscope before use.

Care of the microscope should include keeping it clean. Dust on the optical parts and in the fine mechanical parts is especially bad. The eye tubes should not be left unfilled, nor should the objective turret be left with vacancies. If necessary, extra spaces may be filled with dummy objectives. The microscope should have a dust cover in place when it is not in use. Oil left on plates or on parts of the microscope also catches dust quickly.

When glass plates are repeatedly put on and off the microscope stage, ground glass works into the finely machined parts of the stage assembly causing the metal surfaces to be damaged. It is well to establish a periodic cleaning and checking service for microscopes, just as for typewriters, electric desk calculators, etc.

Sometimes the quality of the image in his microscope may be deteriorating, but so slowly that the scanner does not notice it. Immersion oil that seeps between the components of an objective may have this effect. Objectives should be checked occasionally for such damage.

Emulsion microscopy differs significantly in at least one respect from most other microscopy. This is in the greater emphasis on the third dimension. The microscopy and measurements are always in depth. Searching for events in three dimensions leads to great wear on the fine-focus mechanism. The periodic maintenance of the microscope should include overhaul of these parts. Since the linearity of the  $z$  motion tends to be poorer at the extremes, the scanner should habitually operate the fine focus near the center of its range.

Periodic prism alignment checks are important to maintain scanner eye comfort and morale.



### 7.4 Automatic Methods

Inexperienced people often assume that the scanning would be made easier if the image were projected. It is true that the observer's body would then be less limited in position, but when tried, projection is usually abandoned for the following reasons: (a) the image is always poorer than the virtual image seen through the oculars, and one often needs the best image obtainable. (b) High light intensity is required for projection and this may tend to destroy the emulsion at the focal spot. (c) Extra equipment and more space is required for the scanner. (d) The scanning must be carried out in darkness, which is generally undesirable. (e) It is difficult to provide comfort and at the same time controls as simple and reliable as those on a conventional microscope.

The man-hours required to search for events in emulsion, to count those in a given volume, or to measure track lengths, scattering, and grain density, may be large. This has challenged both amateur and professional designers to attempt to carry out these processes automatically. Blau *et al.* (BRL 50) were among the first to attempt the manufacture of an elaborate instrument for emulsion-track analysis. This machine was designed to integrate the range and to register the optical obscuration of the tracks, but it did not find or count tracks.

The almost universal feeling that automatic electronic methods ought to be applied to the problem of classifying and counting events in emulsion have stimulated numerous attempts to make devices capable of recognition functions. Very little of such equipment now is in routine operation. Some of the reasons are the following: The recognition process, except in some very trivial scanning problems, is seldom simple. Straight and parallel tracks can of course be counted electronically, but various kinds of tracks which scatter, go in many directions, emerge from stars, etc. are almost invariably the types which must be studied in a practical situation. Even straight and nearly parallel tracks offer difficulties. Suppose, for example, that the problem is to find tracks with twice the minimum grain density among a much larger number of minimum tracks.

If the tracks are selected on the basis of the signal received by the obscuration of a slit over the track image, the signal varies rather strongly with depth in the emulsion. The contrast changes with depth because light scatters in the layers of emulsion above the track. The number and the size of the clusters of grains in a track also fluctuates, and segments of minimum tracks are found with as much silver in them as the sparser portions of twice-minimum tracks. If the plate is one that has been exposed to a reasonably high intensity of particles, then often a portion of a second track also may obscure the slit.



The scanning of emulsion must be in three dimensions, which adds an element of complexity. Steep tracks, especially in normally distorted emulsion, also add to the problem.

These remarks, nevertheless, are intended to promote rather than to dissuade the development of practical means for carrying out automatic scanning operations. What should be avoided is a too ambitious approach which leads to immense complexity and ultimate discouragement. The wise procedure, it seems to the writer, is the development of successively better and more generally applicable aids to the human scanner, so that for wider classes of operations the work is speeded up, and increased objectivity is obtained.

Some progress in fact is being made with television scanning. When good television cameras were tested at the Lawrence Radiation Laboratory, virtually all of the microscope image quality was retained, and it was even possible automatically to compensate for changes of image contrast with depth in the emulsion. Track analysis with existing electronic equipment is feasible.

For event recognition, what one may seek is electronic signals with invariant elements that can be used as recognition indices. An obvious criterion that  $n$  discrete grain signals correspond to a track is that their position coordinates correspond to a geometrical line locus in the emulsion. With modern equipment it seems to the writer a definite possibility that the characteristics of many types of events can be encoded, and that automatic tabulation is possible.

Some developments in automatic track recognition and analysis are described in the following references: (BHS 54, BC 54, SL 56, JK 57, G 58.1, RWGL 58, B 60.1, CFLP 59, M 56.1, B 58.2, LBS 50, BKSC 58, TJW 60, VP 60, BC 58, B 60.2, HH 58, WJGR 58, K 56, ZL 60, VMSS 60, OSSW 60, NK 60, G 60, SL 58, MH 58, W 60.2, D 56, BD 57, LBS 50, H 60.1, ACF 56, ACF 57, E 57, S 58.6, K 61.1, W 61.1).

A number of these devices are reviewed in the appropriate chapters of this book. Their philosophy is generally to aid the scanner—not to replace him. They aim to reduce fatigue, to increase speed, and to promote accuracy and objectivity. So long as the cost of the equipment and its maintenance is not greater than the benefits derived from their use, the development of such machines is to be encouraged. One must be on guard, however, against the acquisition of complex equipment which is not completely reliable.

The instruments mentioned above are hardly automatic scanning devices; they are merely pieces of equipment to aid in track measurements. There have been only a few instruments that undertake scanning functions.



An ambitious development of emulsion scanning equipment has been undertaken at the Lebedev Institute, Moscow, by Voronokov *et al.* (VMSS 60). The optical and electronic apparatus used is a complete system to (a) search for tracks having a given direction with automatic advance along such tracks, and (b) to track automatically with periodic readout of the  $x$ ,  $y$ ,  $z$  coordinates, the time,  $t$ , spent between readouts, the change of track direction between readouts, and a multichannel ionization spectrum of the track.

For track direction measurements Cosyns (C 51) built a split-image microscope. One image of a track passing through the center of the field remained stationary and another of opposite symmetry rotated when the system of reflecting prisms was caused to rotate. At any position of the prism system the two images of the track crossed in the field, but at a critical position the two images were superimposed. If the track were straight, the two images of each grain would overlap. Such a device may be useful for coincidence detection of tracks.

A practical system of scanning using an Image Orthicon television camera was developed by Hough *et al.* (HKW 59). The existence of a track is recognized electronically. Delay units are used so that adjacent grains traversed in successive scans produce coincidences defining a track. The device has been used extensively for the routine measurement of particle spectra recorded in a magnetic spectrograph. Nearly parallel tracks well above the minimum of ionization are counted reliably. It is faster than a human scanner by more than a factor of ten. The electronic enhancement of contrast possible by the use of the television camera also enabled Hough *et al.* to increase the speed of human scanning. The scanner then merely watches a television screen for events of the desired type.

Castagnoli *et al.* (CFLP 59) employed an automatic focusing device. It provided remote electromagnetic control of the height of the objective. Such a unit, the Micromag, is made by Wild. They also automatically recorded the photoelectric signal received by a slit superimposed on the track. With a narrow slit ( $0.2 \mu$ ) they measured the pulse height, pulse width, and the integral of the pulse when tracks of heavy ions were traversed by the slit. It was found that the integral was the measured quantity that is most sensitive to the charge of the ion.

Goldsack and van der Raay (GV 56) built an automatic track-counting machine which is able to scan emulsion at the rate of about 2 mm per second and count the tracks with an angular resolution of about  $1/2$  degree. A separate scan is made for each angular setting. Since the depth of focus with a  $45 \times$  Cooke oil objective was about  $30 \mu$ , before processing, considerable tolerance in the dip angle is permitted. The



instrument is said to be capable of counting tracks at the minimum of ionization, even in the presence of strongly ionizing tracks at other angles.

### 7.5 Counting Measurements

Often an experiment can be designed so that the function of the emulsion is simply that of a detector and counting of events is all that is required. The emulsion provides discrimination between various sorts of events and is able to record them all simultaneously. Each can be counted separately.

The ionization of a track may be measured by determining the blob density or by counting gaps and blobs in different length intervals. Delta rays may be counted to help identify the particle producing a track. Energy spectra are determined by counting of tracks in particular range intervals. Angular distributions are determined by counting of tracks in prescribed angular intervals. Prong-number spectra are determined in order to measure excitation energies. Track densities are determined by counting in order to find particle fluxes. These operations and many more may be carried out simply, but a practical knowledge of counting statistics is required in order to know what the reliability of the data is.

Suppose a density of events, presumed to have a uniform average density,  $\langle n \rangle$ , is to be determined by counting. (The density of events may refer to the number of events in a unit of time, length, area, volume, or other quantity which can be divided into equal units.)

If the number,  $n$ , in a particular unit is counted, it will generally not be the same as the number  $n'$  in another identical unit. The average number  $\bar{n}$  found on counting a number of units, however, will approach  $\langle n \rangle$ . Only by counting an indefinitely large number of units would  $\langle n \rangle$  be obtained exactly. For the problem of determining  $\langle n \rangle$  by counting it is important to understand the relationship between particular numbers  $n$  or  $n'$ , the observed mean  $\bar{n}$ , and the expectation value  $\langle n \rangle$ .

The variance is a measure of the statistical spread of  $n$ . Suppose  $n$  is determined an indefinitely large number of times and each value squared. The average value,  $\langle n^2 \rangle$ , of the square of  $n$  is called its mean square value. The variance,  $\sigma^2$ , of  $n$  is  $\sigma^2 \equiv \langle n^2 \rangle - \langle n \rangle^2$ . It is also equal to  $\langle (n - \langle n \rangle)^2 \rangle$ .

The largest variance observed will occur in a random variable,  $n$ , with no constraints.

A Poisson distribution is of this character. In it each countable event occurs with a very low probability, but the number of possibilities



for the occurrence of an event or the number of trials is very great so that a finite density of events is observable. Under these conditions the probability  $p(n, \langle n \rangle)$  for finding a particular number  $n$  of events is:

$$p(n, \langle n \rangle) = \frac{\langle n \rangle^n e^{-\langle n \rangle}}{n!}$$

The variance of  $n$  is  $\langle n \rangle$ . The Poisson distribution is a special case of the binomial distribution. The binomial distribution is the frequency distribution when the probability of the occurrence of an event is finite. Let  $q$  be the probability of occurrence in a trial and the number of trials be  $m$ , so that  $\langle n \rangle = mq$ . Then the probability for a count of  $n$  when the expectation value is  $\langle n \rangle$  can be calculated from:

$$P(n, m, \langle n \rangle) = \frac{m!}{n! (m-n)!} \left(1 - \frac{\langle n \rangle}{m}\right)^{m-n} \left(\frac{\langle n \rangle}{m}\right)^n$$

Its variance, when  $n$  has this distribution, is  $\sigma^2 = \langle n \rangle [1 - (\langle n \rangle / m)]$ .

When  $m$  and  $\langle n \rangle$  are large numbers, the expression for  $P(n, m, \langle n \rangle)$  simplifies to:

$$p(n, \langle n \rangle, \sigma) = \frac{\exp [-(n - \langle n \rangle)^2 / 2\sigma^2]}{(2\pi)^{1/2} \sigma}$$

This is the *normal* or Gaussian distribution. When the distribution is Gaussian the mean absolute deviation,  $\mu$ , of  $n$  from  $\langle n \rangle$  is:

$$\mu = \sigma \sqrt{2/\pi} = 0.7979\sigma$$

In counting measurements this is frequently the most convenient measure of the statistical spread of the data, and it is just as valid as the standard deviation,  $\sigma$ , for determining confidence intervals. The probable error,  $\epsilon$ , which is the deviation that is as likely to be exceeded as not, is found from  $\epsilon = 0.6745\sigma$ .

To obtain a quick estimate of the standard deviation one may find the interval, centered on the mean, in which 68% ( $\approx 2/3$ ) of the values of  $n$  lie. This interval is about  $2\sigma$ . A quick estimate of the expectation value  $\langle n \rangle$  is obtained, when the distribution, like the normal distribution, is unskewed by taking the middle or median value of  $n$ . It is about as valid a measure of  $\langle n \rangle$  as is  $\bar{n}$ .

Suppose  $r$  units are counted and a mean value

$$\bar{n}_r = \frac{1}{r} \sum_1^r n_i$$



is derived from the sum of individual counts,  $n_i$ , of a Gaussian distribution. Suppose also that an estimate  $\sigma_r^2$  of the variance is obtained from

$$\sigma_r^2 = \frac{1}{r} \sum_{i=1}^r (n_i - \bar{n}_r)^2$$

Then a measure of the precision with which  $\bar{n}_r$  measures  $n$  is the standard deviation of the mean,  $\Sigma$ . It is found from  $\Sigma^2 = \sigma_r^2/(r-1)$ . The odds are about two to one that  $\bar{n}_r$  does not deviate from  $n$  by more than  $\Sigma$ . The standard deviation of  $\sigma_r$  itself is approximately  $\sigma_r/\sqrt{2r}$ .

A most important result of statistical theory is the "central limit theorem" (C 46). This states that with certain restrictions the sum of a large number of independent random variables is asymptotically normally distributed. This accounts for the very great importance of the normal distribution in statistics and science, but it is not to be assumed that most distributions are normal or even symmetrical. Skewed and even multi peaked distributions are more nearly the rule in nature. Many special analytic distributions have been studied and tabulated. A type of error that may be introduced by a skewed distribution can be illustrated by a simple numerical example. Suppose it is desired to evaluate the relative frequencies with which two kinds of events, A and B, occur in emulsion, and eighteen events consisting of both types are observed in each of 5 plates. Let the observed numbers be as given in Table 7.5.1.

TABLE 7.5.1  
NUMERICAL COMPARISON OF MEAN RATIO WITH RATIO OF MEANS

Type of event	Plate I	Plate II	Plate III	Plate IV	Plate V	Totals
A	15	14	17	16	17	79
B	3	4	1	2	1	11
Ratio	5.0	3.5	17.0	8.0	17	
Average of ratios:						10.1
Ratio of totals:						79/11 = 7.2

It is readily seen that if the ratio  $n_A/n_B$  is calculated for each plate that the mean ratio, 10.1, exceeds the ratio, 7.2, obtained if the total number of events of type A is divided by the total number of events of type B. Even the latter tends to give an overestimate of the true ratio  $\langle n_A \rangle / \langle n_B \rangle$ .



Because of the skewed character of the ratio distribution, the mean ratio of the two random variables always exceeds the ratio of their mean values. Thus:

$$\langle n_A/n_B \rangle = \frac{\langle n_A \rangle}{\langle n_B \rangle} \left( 1 + \frac{1}{\langle n_B \rangle} + \dots \right)$$

when  $n_B$  has a Poisson distribution.

In order to carry out counting operations in emulsion the field of view must be divided suitably. Several straight lines on the reticle diverging from a common point at the center may be used to define an angular interval for scanning. Straight lines breaking up the area of the field of view into squares or rectangles aid counting operations when there are so many events that they become confusing. By confining one's attention to a sufficiently limited area, the number of events can be made small enough to offer no counting difficulties. For example, to count the single-grain fog background in emulsion is usually difficult unless one divides the field into small areas, and then counts the grains in each area when they come into view as the fine-focus knob is turned.

Counting of blobs in a track may be carried out by superimposing a calibrated reticle scale on the track image. The number of blobs in the scale interval is counted. Then the track is shifted parallel to itself by exactly the length of the scale interval, and a new segment is counted. The segment dip angle (Section 7.6) is also measured so that its true length can be determined. When the track direction changes sharply at a point, counting is carried out to that point, but then the scale is rotated so as to remain parallel to the track and the new dip angle is measured.

In track counting, if there is the possibility, as there usually is, that tracks with certain directions are detected with lower efficiency than others, tests can be made to reveal the effect. If all azimuth angles are equally probable then plotting frequency versus azimuth will disclose a deficiency of certain azimuth angles. If all directions in space are equally probable, then plotting the numbers found in equal intervals of the sine of the dip angle will disclose any bias in dip angles. Secondary track directions are expected to be distributed uniformly around the direction of an incident unpolarized beam, so that a plot of frequency versus angle around the beam axis may reveal other biases. For a beam parallel to the emulsion surface this may also test the correctness of the shrinkage factor used, as will the dip-angle-distribution test. Certain other scanning biases may be revealed by comparison of the frequency with which tracks are observed to enter each of the eight octants around the origin.



## 7.6 Geometric Measurements in Emulsion

Geometric measurements in emulsion consist of determining the coordinates of points in a suitable coordinate frame, measurement of distances between points, measurement of areas and volumes, measurement of projected and space angles, measurement of statistical deviations of a track from a straight line, applying tests for coplanarity, collinearity, and symmetry, measurement of angular and spacial distributions, and, with recent development of high magnetic field techniques, measurement of track curvature.

These measurements should be made with a full knowledge of the effects of emulsion distortions discussed more fully in Chapter 6. It is necessary also to know how to make geometric corrections for scattering of tracks out of the emulsion, and for losses of particle flux arising from interactions and decay.

For geometric measurements it is essential that the eyepiece reticle should have engraved on it a scale which divides the useful field diameter into parts, preferably 100. This useful diameter is perhaps 70% of the extreme field diameter, and may be taken along one axis of an inscribed square. For ease in using the reticle, every tenth division should be perhaps 3% of the field in length, the intervening fifth divisions should be about 2% of the field, and the others may conveniently be about 1% of the field in length. At a magnification of 1000, a division of the field will then be in order of magnitude  $1\ \mu$ . (See Fig. 7.2.2)

Coordinates of points in the field can be measured using such a reticle with standard deviations of less than a micron.

Angles are defined as follows: an angle  $\theta$  of a track is defined to be the angle to the direction of particle motion measured counterclockwise with respect to the  $x$  axis in the plane of the emulsion. This is called the azimuth angle. The dip angle,  $\delta$ , for a track is the angle between the track in unprocessed emulsion and its own projection on the surface of the emulsion, taken positive when the direction of the particle motion is upward and in the direction of increasing the  $z$  coordinate (right-handed  $x, y, z$  coordinate frame). The angular coordinates also can be utilized to describe the  $x, y, z$  coordinates of a point relative to an arbitrary origin as follows:

$$\begin{aligned}x &= r \sin \theta \cos \delta \\y &= r \sin \theta \sin \delta \\z &= r \cos \theta\end{aligned}\tag{7.6.1}$$



The space angle  $\chi$  between two lines or tracks having azimuth and dip angles  $(\theta_1, \delta_1)$  and  $(\theta_2, \delta_2)$  is calculated from the measurements as follows:

$$\begin{aligned}\cos \chi &= \cos \delta_1 \cos \delta_2 [\cos (\theta_2 - \theta_1) + \tan \delta_1 \tan \delta_2] \\ &= \frac{\cos (\theta_2 - \theta_1) + \tan \delta_1 \tan \delta_2}{[(1 + \tan^2 \delta_1)(1 + \tan^2 \delta_2)]^{1/2}}\end{aligned}\quad (7.6.2)$$

The reason for giving the second form of this equation is that  $\tan \delta$  is the quantity that is directly measured with the microscope.

Errors in the measurement of geometric quantities such as the space angle are treated best by considering the elementary measurements that go into the determination. If possible the quantity treated should have a Gaussian distribution of measurement errors. The angle  $\theta$  is a quantity of this sort. Usually it can be measured with a standard deviation of somewhat less than one degree, although this varies considerably with the amount of track scattering and the grain size. The angle  $\theta_2 - \theta_1$  will then have a Gaussian distribution of error with twice the variance of a single angular measurement. The measurement of  $\tan \delta$  depends essentially on the measurement of two  $z$  coordinates, and its variance will therefore reflect twice the variance of one measurement, but the distribution of the error is expected to be Gaussian. The quantity  $\tan \delta$  can usually be measured with a standard deviation no better than about 0.01, but it may be much worse under poor conditions of measurement.

Heughebaert and Heughebaert (HH 58) have refined the measurement of small  $z$  displacements by varying the eye-tube length. By calibration, the change in the object distance for a given change in the image distance was found, and a very large multiplication obtained ( $\approx 10^4$ ).

The angle coordinates we have adopted for emulsion, Eq. (7.6.1), may be easier to remember if it is noticed that they are the same as the geographic coordinates of a point. The angle  $\theta$  is analogous to the East Longitude and  $\delta$  corresponds to the North Latitude.

The reticle is used in several ways. A straight line crossing the field is used to help the eye pick out grains forming a straight track of low grain density. By placing the straight line on top of a track so as to obtain the best possible alignment with the track, its azimuth direction with respect to a fixed direction or to the direction of another track may be determined. This is done by means of an eyepiece goniometer. The goniometer is usually divided into  $360^\circ$ , perhaps with a vernier and magnifying lens so that tenths of degrees can be estimated. It is convenient to adjust it so that when the goniometer is set at zero, the stage motion along the  $x$  axis is accurately parallel to the straight line on the



reticle. Then the angle  $\theta$  will be read directly from the goniometer.

The measurement of the  $z$  coordinate is complicated by the fact that gelatin shrinks in processing and its index of refraction is not unity. When immersion oil of the same index as the gelatin is used, however, the displacements of the objective between the positions where two grains with the same  $x$  and  $y$  coordinates are in sharp focus is equal to the difference of their  $z$  coordinates. This displacement of course must be corrected for the emulsion shrinkage to obtain the original displacement. When a dry lens of large aperture is used, one should relate the  $z$  displacement of the lens and the difference of the  $z$  coordinates between two objects by calibration.

To measure dip angles, one must take account of the fact that the surface of best focus in the field of view is not a plane. If the optics are good the surface will have symmetry about the microscope axis so that two grains seen in focus equidistant from the center will have the same  $z$  coordinate.

Using this assumption, one measures the dip angle of a straight segment of track as follows: the segment is centered in the field; one end is brought into focus and the  $z$  coordinate read (this should be done with the objective being raised). The reading is repeated on the other end of the segment, and the projected length,  $L$ , of the segment is observed on the eyepiece scale. Sometimes systematic errors can be reduced by measuring each  $z$  coordinate in the emulsion relative to the glass-emulsion interface, but then the statistical error of the dip-angle measurement is doubled, and this practice is not recommended unless good reasons for doing it are known. It is assumed that the original thickness,  $T$ , of the emulsion layer has been measured (see Chapters 4 and 6). One also observes the difference,  $t$ , between the  $z$  coordinate reading at the surface of the emulsion and at the glass-emulsion interface. Then the shrinkage factor,  $S$ , is  $T/t$  and the true dip angle,  $\delta$ , is found from  $\tan \delta = (T \Delta z)/(tL)$ , where  $\Delta z$  is the observed difference in  $z$  coordinates between the ends of the track segment. (The angle  $\delta$  is positive if the  $z$  component of the particle velocity is positive.) The length of the track segment is  $L \sec \delta$  or  $[L^2 + (\Delta z T/t)^2]^{1/2}$ .

When certain objective lenses are used it will be found that the magnification varies with the distance from the center of the field. Using a uniformly ruled eyepiece reticle, an object near the edge of the field may appear shorter than when at the middle by as much as 1 or 2%. This is an unacceptable error for some kinds of measurements, and either an objective without this fault must be used or a correction made for the error, which is usually a quadratic function of the distance from the center of the field.



There are two common methods for calibrating the eyepiece reticle. One method is to employ a stage micrometer obtainable from optical supply houses. Such a micrometer is usually a piece of glass on which are ruled parallel lines of known spacing perhaps 10 and 100  $\mu$  apart. When the image of the stage micrometer scale is superimposed on the reticle, a calibration of the reticle for that particular objective lens and total eye-tube length (this depends on the interocular distance) can be made. For good accuracy commercial stage micrometers have frequently been found insufficiently uniform, or systematically in error, so that one may be wise to use more than one micrometer from different sources for comparison.

Another method for calibrating the reticle or a portion of the reticle scale is to measure off a large known distance in units of the reticle scale. This may be done if the stage can be displaced accurately and controllably from one end to the other of the standard length, or if the screw moving the stage has an accurately known pitch. Unless the screw is perfectly straight, a screw-driven stage will have a periodic error that may be quite large. An integral number of screw rotations is suggested for obtaining a known displacement of the stage. The necessity for a  $z$ -coordinate calibration of the microscope is reduced if the system of measurement described above is used, but it is in any case necessary to establish that the fine focus calibration does not vary through its focal range. This is a large error for some microscopes. The  $z$ -coordinate calibration is carried out by obtaining a piece of glass having an accurately known thickness of about 200  $\mu$ , and an index of refraction closely matching that of the immersion oil, perhaps 1.515. Fine scratches or tiny bits of opaque matter should be visible on both surfaces of the glass so that one can focus successively on the top bottom surface using an oil immersion objective. With the number of turns of the fine focus knob from one extreme of its motion as the abscissa, one can prepare a calibration curve for the  $z$ -coordinate giving the number of microns per  $z$ -scale division as the ordinate scale.

In addition to geometrical measurements, time can be measured in emulsion by combining the measurement of velocity and distance. The proper time,  $dt^*$  (see Chapter I, Volume II), required to traverse a distance  $dx$  is

$$dt^* = \frac{dx}{v} \left( 1 - \frac{v^2}{c^2} \right)^{1/2}$$

Here  $v$  is the particle velocity and  $c$  the velocity of light.



The proper residual time  $T^*$  for a particle to come to rest, or the moderation time, is calculated from

$$T^* = \int_0^R \frac{dR}{v} \left(1 - \frac{v^2}{c^2}\right)^{1/2} \quad (7.6.3)$$

where  $R$  is the residual range.

A common problem is to determine the decay rate or mean life of unstable particles in emulsion. For the analysis of the data it is usual to apply the statistical method of "maximum likelihood" which will now be outlined.

Suppose that the probability for a measurement of a quantity  $t$  to be in the interval  $dt$  is known to depend on a parameter  $\lambda$  which it is desired to estimate. Then one can obtain the probability distribution of  $\lambda$  and the most probable value of it from  $n$  measurements,  $t_i$ , of  $t$  if the distribution function is  $p(t, \lambda)dt$ , both as a function of  $\lambda$  and of  $t$ .

One constructs a function  $P(t_1, t_2, \dots, t_n; \lambda)$  that expresses the joint probability for the  $t_i$  to be found in particular intervals  $dt_i$ .

This is:

$$P \prod_{i=1}^n dt_i = \prod_{i=1}^n p(t_i; \lambda) dt_i, \quad \text{or} \quad P = \prod_{i=1}^n p(t_i; \lambda) \quad (7.6.4)$$

This function of  $\lambda$ , normalized so that  $\int p d\lambda = 1$ , is the probability distribution of  $\lambda$  if no a priori bias exists in the distribution of  $\lambda$ .

The maximum likelihood estimate of  $\lambda$  is then found from the solution of

$$\sum_{i=1}^n \frac{1}{p(t_i, \lambda)} \frac{\partial p(t_i, \lambda)}{\partial \lambda} = 0 \quad (7.6.5)$$

The uncertainty of the result can be obtained from the second derivative of  $P$ .

To apply Eq. (7.6.5) to the decay-rate problem (B 53.2) suppose that  $n$  similar unstable particles are observed to decay. Let the  $i$ th particle decay at a proper time  $t_i$  after the observation began. Had it not decayed, the observation would have been continued for a total proper time duration of  $T_i$ , which perhaps might be the moderation time of the particle in emulsion. The decay being governed by the radioactive decay law, one assumes that

$$p(t_i, \lambda) dt_i = \frac{\lambda e^{-\lambda t_i} dt_i}{(1 - e^{-\lambda T_i})} \quad (7.6.6)$$



so that

$$P = \lambda^n \left[ \exp \left( -\lambda \sum_{i=1}^n t_i \right) \right] \prod_{i=1}^n (1 - e^{-\lambda T_i})^{-1} \quad (7.6.7)$$

This expression may be plotted as a function of  $\lambda$  to display the probability distribution. To determine the maximum analytically, it is simplest first to take logarithms:

$$\ln P = n \ln \lambda - \lambda \sum_{i=1}^n t_i - \sum_{i=1}^n \ln (1 - e^{-\lambda T_i}).$$

Then on differentiating

$$\frac{n}{\lambda} - \sum_{i=1}^n t_i + \sum_{i=1}^n T_i (e^{\lambda T_i} - 1)^{-1} = 0. \quad (7.6.8)$$

The solution of this equation for  $\lambda$  is the one of maximum likelihood.

In emulsion it is simplest to study distribution of projected track angles. This distribution can be obtained from the spatial distribution quite simply if, as is common, there is axial symmetry. It is also desirable to know how to find the spatial distribution when only projected angles were measured.

Suppose that the probability for the track to lie in the interval  $\mu$  to  $\mu + d\mu$  is  $-(1/2)F(\mu)d\mu$ , where  $\mu = \cos \chi$ ,  $\chi$  being the angle to the axis. We wish to find the probability  $p(\nu)d\nu$  that  $\nu$  lies in the interval  $d\nu$  when  $\omega (= \arccos \nu)$  is the track angle projected on a plane containing the axis of symmetry. Then

$$p(\nu) = \frac{1}{\pi\nu(1-\nu^2)^{1/2}} \int_0^\nu \frac{F(\mu)\mu d\mu}{(\nu^2 - \mu^2)^{1/2}} \quad (7.6.9)$$

As an example, one may calculate the projected angular distribution of the protons that recoil from  $s$ -wave neutron collisions (see Chapter 6 in Volume II). Then  $F(\mu) = -4\mu$ . On making this substitution in Eq. (7.6.9), the projected distribution is found. It is

$$p(\nu) = -\nu/(1-\nu^2)^{1/2} \quad (7.6.10)$$

When it is desired to know the angular distribution  $\rho(\omega)d\omega$  rather than the distribution of the cosine of the projected angle, one calculates it as follows:

$$\rho(\omega) = p(\nu) d\nu/d\omega \quad (7.6.11)$$

so that  $\rho(\omega) = \cos \omega$  for the recoiling protons.



On the other hand, suppose  $p(\nu)$  or  $\rho(\omega)$  has been measured, but it is the distribution function  $F(\mu)$  that is wanted. This situation is treated as follows:

We put  $\nu^2 = x$ , and write  $2\pi\nu(1 - \nu^2)^{1/2}p(\nu) = f(x)$ . We also put  $\mu^2 = \xi$ , and write  $2F(\mu)\mu d\mu = u(\xi)d\xi$ . Then Eq. (7.6.9) becomes a standard form of Abel's integral equation:

$$f(x) = \int_0^x \frac{u(\xi) d\xi}{(x - \xi)^{1/2}} \quad (7.6.12)$$

This equation can be inverted. The result is

$$u(x) = \frac{1}{\pi} \frac{d}{dx} \int_0^x f(\xi) (x - \xi)^{-1/2} d\xi \quad (7.6.13)$$

Equation (7.6.13) is the complete solution for the problem of finding the spatial distribution when the projected distribution is known.

On setting  $\mu = \cos \omega \cos \lambda$ ,  $F(\mu) = g(\cos \omega \cos \lambda)$ . Then Eq. (7.6.9) can also be written

$$\rho(\omega) = \frac{1}{\pi} \int_0^{\pi/2} g(\cos \omega \cos \lambda) \cos \lambda d\lambda \quad (7.6.14)$$

## 7.7 Area and Strip Scanning

The most knowledgeable scanning probably is carried out by observers of much experience when first scanning an emulsion stack or plate in which new things are to be expected. Such an investigator may look quickly at everything hoping to find something with which he is unfamiliar. Events of this sort often are worthy of further study.

Most scanning, however, is carried on as part of a planned program, in which events of certain types are sought in a systematic way. Area scanning of a pellicle is usually done in strips equal in width to a side of an inscribed square in the microscope field of view. The procedure is to cause the focal surface in the emulsion to sweep up and down from the surface of the emulsion to the glass by rolling the fine focus control between the fingers while observing the events successively coming into and going out of view. One such elementary motion down or up can be called a scanning traverse. Before shifting the field, more than one traverse may be made. For high efficiency the field must be divided into a number of separate areas each sufficiently small so that the whole of the area can be apprehended as the traverse is made. Then scanning traverses are made as successive areas are examined, and the field is not shifted



until all the area has been searched. The most rapid scanning procedure is to execute a scanning traverse, shifting the field by the width of the inscribed square, make a traverse in the opposite direction, shift the field, make another traverse, etc. The volume of emulsion scanned in this way is equal to  $nw^2T$  where  $n$  is the number of scanning traverses,  $w$  is the width of the inscribed square, and  $T$  is the preprocessed emulsion thickness. Even at a magnification as low as 100, however, it is usually possible to scan only about 0.2 or 0.3 of a cubic centimeter per hour in this way, and most scanning tasks go much slower. It is because of the large number of man-hours required to carry out area scanning (really *volume* scanning) that means to increase the scanning speed are sought. One approach is to increase the scanning speed at the expense of the efficiency. So long as the product of the efficiency and the scanning speed is rising one may increase production by increasing the scanning speed. It is even possible to do quantitative work in this way if care is taken to determine scanning efficiencies accurately.

When area scanning is directed toward finding the termini of tracks which are more or less parallel in the emulsion, then the strip that is being scanned should be parallel to the tracks and the motion of the stage should be such that each track is followed in the direction of particle motion to its terminus. The presence of a track signals its imminent termination before the actual end is seen and the scanning efficiency is improved. If the track leaves the prescribed strip before stopping, one does not attempt to follow it, because it will be picked up in the next strip. This "no deviation" rule is not necessarily maintained when one is scanning for extremely rare tracks.

Some general observations can be made about measurement of area scanning efficiency, and the adjustment of scanning rate to increase the over-all production rate. The statements must be mostly qualitative, however, because a thorough study of these problems, while much needed, has not been made. Let the area scanning problem be the mere finding of events of a specified type in a given volume of emulsion—measurements on the events are not considered part of this restricted interpretation of "scanning."

In the following, such area scanning problems are broken down into classes and the scanning procedure for each class discussed.

*Class A.* The nature of the problem requires that *all* the events of a certain type in a given volume of emulsion be found.

This kind of problem may arise if only a limited number of events are available and nothing is known about what features of the event determine the probability that it be found.



The usual procedure in this case is simply for an observer to scan the volume and record a number  $N_1$  of events, then to scan it again by the same method recording a number  $N_2$ . If either sample contains events not found in the other, the scanning must be repeated until no new events are found. Then the scanning technique, the microscope magnification, and the observer may be changed to determine whether any further events can be found.

*Class B.* It is required that the number and an unbiased spectrum of events in a given volume be found.

Suppose, for example that the problem is to find the total number of neutron-produced stars and their prong spectrum, when the chance of missing an event depends on its prong number.

If one has no prior knowledge of the spectrum, the volume should be scanned once by a given observer, and a spectrum  $S_1$  of events recorded. The same observer should again scan the volume and another spectrum of events,  $S_2$ , will be found.  $S_2$  will generally contain both new events and events that were found before, while  $S_1$  may contain some events not found in  $S_2$ . The events found only in  $S_1$  form a spectrum, those found only in  $S_2$  form another spectrum which should be similar to the first. The events common to  $S_1$  and  $S_2$  also form a spectrum which may have a different shape from the others if stars with certain prong numbers are easier to find than others. Now suppose the volume scanned actually contains  $N_i$  stars with  $i$  prongs, and the observer has an efficiency,  $E_i$ , for finding stars of  $i$  prongs. Then if the number of events of  $i$  prongs found in the first scanning is  $N_{i1}$ , in the second scanning  $N_{i2}$ , and the number common to both scans  $N_{i12}$ , then:

$$N_i = \frac{(N_{i1} + N_{i2})^2}{4N_{i12}}$$

and

$$E_i = \frac{2N_{i12}}{N_{i1} + N_{i2}}$$

The expected equality of each pair,  $N_{i1}$  and  $N_{i2}$ , should be used as a check. The results can also be verified by another observer, and by altering the technique. The efficiencies may then change, but the  $N_i$  should remain statistically constant. It is essential in this example that the only important variable affecting the efficiency be the prong number. In particular, prongs at minimum ionization may sometimes be present, but if the emulsion records minimum tracks with difficulty or not at all, then the derived prong spectrum will be distorted.



*Class C.* The problem requires that a representative sample of events be found.

In this case it is not necessary to choose a scanning technique that insures that all the events are found—it is necessary only to select recognition features which do not introduce bias.

A representative sample of  $\pi$ - $\mu$ - $e$  decay chains can be found by simply recording pions stopping and decaying into muons. If it is required in addition that the muon be seen to stop, that would bias the result, because one would in that way select events with muons tending to have small ranges.

For speed of scanning, generally a low magnification is indicated. Only sufficient magnification is required to recognize the events and to avoid the confusion of too many events in a field of view. Only one focal traverse of each field of view is justified.

*Class D.* The scanning problem is to obtain a sample of a particular kind of event.

Here the most rapid and certain procedure is to record events which have any feature or combination of features which uniquely identifies the event. If the population from which the sample is to be taken is virtually infinite, as it often is, it is unnecessary to attempt to identify difficult events or to risk their misidentification. The sole goal is to find the maximum number of genuine events in a given time.

For example, suppose it is desired to investigate the grain density as a function of residual range for negative  $\pi$  mesons in a particular emulsion stack. One would then presumably select for investigation tracks which scatter and change in grain density on stopping like  $\pi$  mesons, and which in addition terminate in a star. The scattering and grain density variation, which are observed in a glance at the track, identify it as a  $\pi$  or  $\mu$  meson. The star indicates that it is a negative meson, and also that it is probably a pion. If there is a large possible contamination of negative muons, it would be necessary to require that the visible energy release in the star exceed an arbitrary figure such as 30 Mev. By this method one loses pions which interact with little visible energy release, and probably obtains a biased sample with respect to its energy spectrum at production. These biases, however, are irrelevant to the question under investigation.

*Class E.* This is a variation of area scanning known as strip scanning or edge scanning. This might be done, for example, if a stack of emulsion is exposed so that a beam of particles enters one face nearly perpendicularly, and so that the tracks lie essentially in the plane of the emulsion.



Then one may wish to know the density and distribution of the beam entering the stack, or he may wish simply to find tracks of a specified type to be traced into the stack.

The procedure then might be to traverse each plate parallel to the leading edge and perpendicular to the incoming tracks. Because of the edge distortion and blackening this usually must be done at least a millimeter in from the edge. Often such a scanning operation must be discriminative. Only tracks of a particular grain density may be sought. Sometimes also the distribution of the angles at which the tracks enter the edge may be useful information. Perhaps one wishes to study the track density and angular distribution as a function of distance along the edge. The process of scanning then would be to make a focal traverse at a point near the edge at one end of the interesting interval, recording the direction and coordinate along the edge for each track of the desired type. Then the plate would be shifted parallel to its edge the width of one inscribed square in the field of view, and the process repeated.

### **7.8 Photomicrography of Particle Tracks**

The track that a particle leaves in emulsion is an extended three-dimensional object. While its length may be measurable in macroscopic units such as centimeters, its width is normally about  $1\ \mu$ . The developed emulsion grains, a linear array of which constitute the track, have diameters that are about equal to a wavelength of visible light. The magnification needed to photograph the track is, therefore, very high. The depth of field in which grains will be in focus is at most a few microns. The disparity of its dimensions is so great that the photomicrography of a track presents a difficult problem.

One method of photographing emulsion events is to make many photographs of the same field adjusting the focal plane between exposures by an amount equal to the depth of focus. This is done most efficiently by making use of the  $z$ -axis calibration of the microscope.

It is necessary that the microscope-camera assembly be stable so that in spite of the handling required to shift the film, etc., the surface that is in focus is determined solely by the reading on the fine focus knob. Prior to starting the series of exposures the  $z$ -axis readings of the highest and lowest points of the track or event are determined. Then starting at the bottom or top, photographs are made at a precalculated series of  $z$  settings so that evenly spaced sections through the event are photographed. The photography can be carried out rapidly because there is no necessity to look at the event while making the photographs.



Each negative, or merely the portion of it that is in focus, is then contact-printed on hard surface paper. The areas of paper containing sections of track in focus are then cut out with a scissors, and, employing identifiable grains or other background events for matching, the segments are pasted together to form a continuous track. When these are mounted on cardboard or some other base material and rephotographed, the resulting representation of the nuclear-track event is known as a photomontage.

The preparation of a photomontage may be very tedious, especially when the event is complex, so that other methods of reproducing the three-dimensional event in two dimensions have been utilized. For example, the event may be traced in projection. In this method one projects the image of the event on paper and draws in all grains in focus. Then as the focus is gradually changed each new grain coming into focus is traced on the paper.

P. Demers (D 58) has developed an ingenious method of compressing the information in a track into a smaller space. In effect, he photographs the track with less magnification along the track than perpendicular to it. In this way the scattering is accentuated, and the terminal portions of the paths of particles differing in mass are distinctly different in appearance.

A flat field is more needed for photomicrography than for track scanning and a special effort to obtain an objective-ocular combination giving a flat field is justified. The maximum resolution and contrast in the photographs is also important. Objective lenses of high N. A. with matching condensers should be individually tested to obtain the best one. The type of film used for microfilming with development in D-11 provides good contrast for photomicrography and paper of No. 3 grade or higher should be used for printing. To obtain the right exposure, tests must be made, and once the best conditions are established it is wise to record the light emerging from the eyepiece lens by a photocell that collects all the light. If this light intensity is reproduced with other light sources, emulsion plates, or objective lenses, one may continue to obtain the correct exposure without further time consuming tests.

Ordinarily the relocation of an event for photomicrography is very simple if the emulsion has a grid printed on it. Then one merely records the coordinates of the event when it is to be photographed. When no grid is available, a method of relocation has been developed by Baitz (B 58.4). He utilizes a piece of thin diazo film taped to the surface of the plate. The microscope condenser and lamp diaphragm are adjusted to give a very small spot of light illuminating the event. After an intense light exposure the diazo film can be developed in ammonia fumes, the illuminated spot remaining transparent while the rest of the film is rendered opaque.



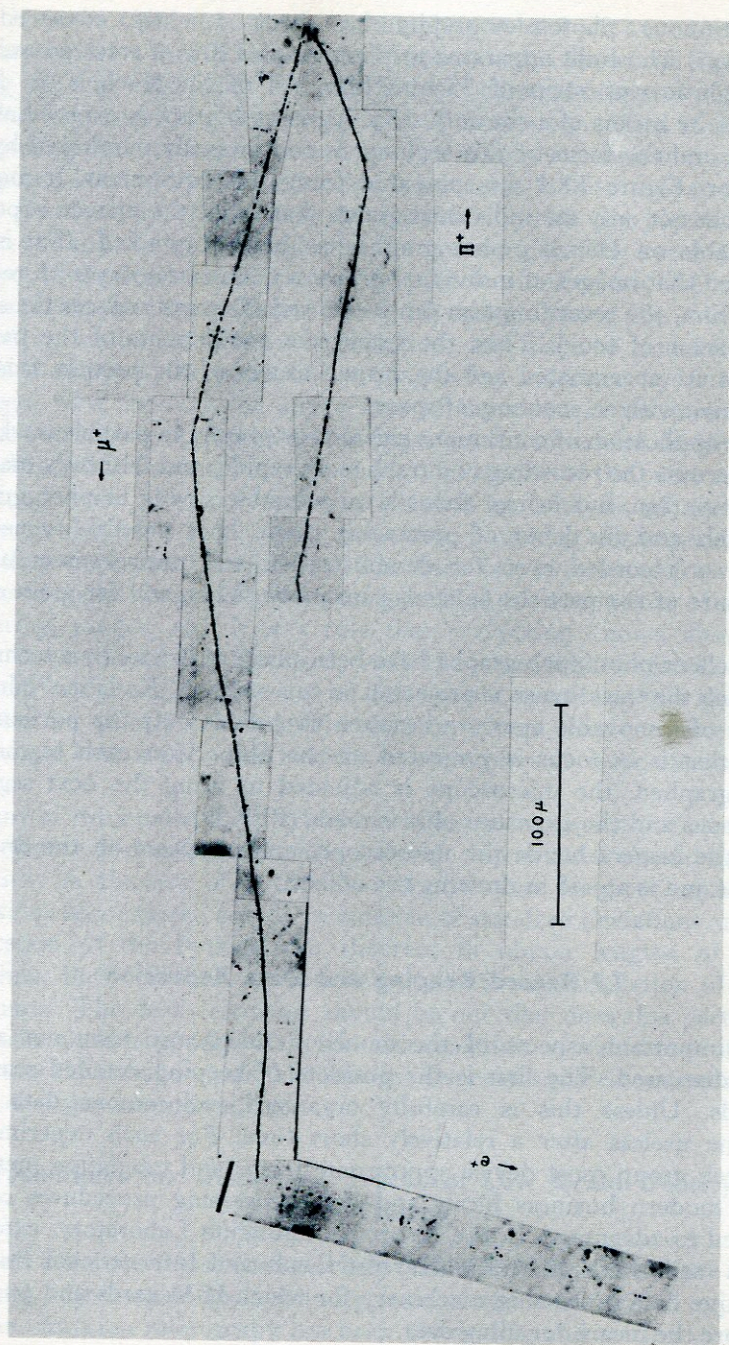


FIG. 7.8.1. Photomicrograph of  $\pi^+\pi^-\pi^0$  decay made using continuous photomicrographic equipment. (Photomicrograph by R. Blinkenberg.)



Continuous photomicrography has been recently advanced by A. Oliver, who built apparatus to photograph  $120\ \mu$  of track per minute on a continuous strip of 35 mm film. All of the track is in focus because by means of a slit only a  $2\ \mu$  segment of track is exposed at any instant and the focus of this segment is continuously monitored by the operator. Figure 7.8.1 was prepared using this equipment. It may be seen that not only are individual grains sharp, but the uneven exposure observable on Demer's photographs has been eliminated. If it is not required that images of individual grains remain stationary with respect to the film, the recording film can be slowed (Demers reduces the speed by a factor of four). Then the transverse components of the particle motion are accentuated and the main features of the particle behavior are shown with an economy of space.

The application of continuous photomicrography to particle tracks not only permits the recording of a track more rapidly and faithfully than the photomontage, but brings about a considerable saving in photographic materials and the labor of processing them. It is possible to use the tracks so recorded even for demonstration and measurement of the curvature of the particles in strong magnetic fields, and for grain counting.

Excellent photomicrographs have been made at Bristol by a technique in which the track image is projected on to a strip of "Kodakline" film. By means of a movable aperture between two slides only the portion of a track that is in focus is projected on the film. After each segment is photographed, the microscope is adjusted to bring the next segment into focus and the exposure of it is made (PFP 59).

In the camera lucida the microscope image appears on the drawing surface and is an aid in drawing the object.

### 7.9 Record Keeping and Data Reduction

Two important aspects of the emulsion microscopy have not as yet been discussed. The first is the problem of keeping detailed scanning records. Unless this is carefully organized, voluminous data often become useless after a relatively short time. For each experiment a research group must devise appropriate forms and tabulation methods. Here modern business forms and data processing procedures can be utilized to advantage. In the Lawrence Radiation Laboratory, extensive use is made both of McBee Keysort Cards and International Business Machine data processing machinery for which IBM cards and punched tape are the means for filing data.



A Keysort Card constitutes a complete record of an event. The information on a card is cumulative. Such a card is shown in Fig. 7.9.1. Along the top edge holes are punched out corresponding to the most obvious facts regarding the event, and only those are punched at the time of scanning that are known to be true. For example a minimum ionizing star prong is not punched " $\pi$ " unless it has actually been proven to be a pion. On the face of the card the scanner's initials are placed at the upper left and the event number at the upper right. The event number consists of the stack identification, the pellicle number, and the number of the event in that pellicle. The grid square where the event was picked up in the case shown is indicated, and also the grid square in which it stopped, the point of stopping being indicated by a dot. An enlarged view showing the appearance of the event in the microscope field is also shown. Adjacent to this figure are the initials of the physicist who checked and concurred with the interpretation of the event and the punching made. Further space is allotted for analysis of secondary tracks on the front face; along the sides, punching corresponding to secondary track data is continued. The back face is reserved for various rubber-stamped forms. They contain detailed measurements of angles, scattering, ranges, etc. It is a rule that everything known about the event is contained on the card, and the classifiable information is punched in the edges. Then out of many cards, just those of a specified type can be quickly selected. The data on a card may continue to be augmented over a period of months or even years as more analyses are made.

Many of the smaller data reduction tasks can be carried out by means of an electric desk calculator and a slide rule; the scanner should become proficient in the use of both. Two of the most frequent arithmetic operations encountered are the calculation of standard deviations and the application of the Pythagorean theorem to obtain lengths of track segments. Both of these operations require the accumulation of sums of squares. The desk calculator should be one that does this particular operation simultaneously with the accumulation of the sums of first powers of the numbers punched into it. A special square-root extracting desk calculator saves time also.

### **7.10 Techniques for Discerning Tracks of Low Grain Density and Track Tracing**

Because even the best commercially available emulsions have been marginal with respect to sensitivity, one of the most skilled types of work in emulsion microscopy has been the finding and tracing of tracks







$\Sigma$   
 RANGE \_\_\_\_\_ (g) .740 (corr)  
 Op at K \_\_\_\_\_ (corr)  
 Op at end \_\_\_\_\_ (corr)  
 $\Delta$  at K \_\_\_\_\_  
 $\Delta$  at end \_\_\_\_\_  
 T \_\_\_\_\_  
 E \_\_\_\_\_  
 pc \_\_\_\_\_

r at K \_\_\_\_\_  
 r at end \_\_\_\_\_  
 r to end  $29.0 \times 10^{-12}$

PRONG	RANGE	OR	Z <sup>A</sup>	T	$\Theta$	Tan $\delta$
1	873 $\mu$		H <sup>+</sup>	13.0 MEV		
2	42 $\mu$		HF	2		
3	4 $\mu$		?	?		

Total = 23 Mev

Hyp. FRAG DATA:

	RANGE	tan $\delta$	$\Theta$	p $\beta$	I	Ident.	T	pc
F						<sup>A</sup> He (sure)		
1	22.481 $\pm$ 2.81	+7.784 $\pm$ .0284	309.4 $\pm$ 5			proton	82.78	402.72
2	20.587 $\pm$ 2.57	-7.643 $\pm$ .0283	121.9 $\pm$ 5			"	78.11	392.29

1 and 2 are not colinear. Are definitely protons

Only  $\text{He}^4 \rightarrow p + p + n$  feasible with  $8E \leq 9.72 \pm .88$

space angle =  $174^\circ$

used to record data on  $K^-$  meson interactions (IDLRL).



at the minimum of ionization. A good test of scanner acuity is the ability to discern a minimum track in single-grain fog.

One type of problem is the finding of a near-minimum track suspected to originate at the end of another track, as for example the track of a secondary pion from the decay of a sigma hyperon. An experienced scanner might treat this situation as follows: the terminus of the hyperon is placed in the center of the field, and if a preliminary look around the field reveals no radial row of grains in the focal plane of the track end, it is assumed first that the track is dipping downward. While rapidly rotating the focusing knob so as to move the objective up and down about  $50\ \mu$  relative to the emulsion, he looks in each octant in turn for a track radiating from the center. Because the objective is moving, a dipping track, only a small portion of which can be seen in focus, will give the impression of darting out from the center as the objective is moved down, and to approach the center as it is moved up. After carefully examining each lower octant in turn, the scanner directs his attention to the upper four octants. Now when the objective is raised the track will appear to shoot from the center and vice versa. If something is found, but its identification as a track is uncertain because only two or three aligned grains are seen, a reticle line should be superimposed on the grains, and further grains sought on the continuation of the line. The  $z$  coordinate, of each successive grain should, of course, vary linearly with the radial distance from the center.

If a track is definitely found, the next task is to be certain that it originated at the hyperon ending or other event which is supposed to have given rise to the track. The scanner asks critically if it lines up exactly with its supposed origin both vertically and horizontally. He must also check along the reticle line to be sure that the track does not extend on the other side of the supposed origin.

Another type of work involves following a minimum track. The difficulties arise because the grain spacing varies statistically and there is always a single grain background throughout the emulsion volume. There will also be other confusing tracks—both straight tracks of fast particles, and the tracks of low-energy electrons. All of these make it difficult to discern a track of low grain density. One aligns the reticle with the track and notes its dip angle, perhaps as much by feel of the fine-focus control and the length in focus as by measurement. It is said that in following a track one must not look for it too closely or he will not see it. The eye follows the track along the diameter of the field to the edge of the field of view, and it is then left in focus while it is translated to the other side of the field, where it should again be in focus, even if the field is dished. With the aid of the reticle aligned with the



track, it is again followed across the field of view. This is repeated until the track leaves the pellicle or terminates. If a good grid (Chapter 4) is printed on the pellicle, careful notation is made of the grid square and the point in the grid square where the track leaves the pellicle. A standard printed form for this notation is useful.

Of great importance for tracing the track, whether or not one has a grid, is the presence of nearby heavily ionizing steep tracks that can be identified in the next pellicle. Before leaving a pellicle, the  $x$  and  $y$  distances of the track exit point from such landmarks are recorded, and the dip and azimuth direction of the track noted.

The grid, while very useful, cannot be located on the pellicle closer than a thousandth of an inch or so by present methods. It is also printed on only one surface of the pellicle and therefore can be displaced by shear distortions. For these reasons steep, heavily ionizing tracks are the best guides for the alignment of two adjacent pellicles. Certain types of emulsion distortion may cause difficulties, and if a large air gap exists between pellicles as much as 2 or 3 mm of a flat track may be lost. Distortions caused by blisters in the emulsion are particularly troublesome, but if the presence of a blister is known, one will exercise especial caution in tracing a track through this region. With reliable guideposts and assuming a continuity of track direction in three dimensions, usually the track can be picked up on the next plate without great difficulty. A skilled scanner sometimes may even skip whole pellicles in rapidly tracing a track through the stack. The highest magnification is not necessarily recommended for tracing minimum tracks because often then too few grains are contained in a field of view. A  $20\times$  oil objective with  $16\times$  wide-field oculars may be very useful for such work if the background of single grains and tracks is low enough so that the depth of focus is not important for track discernment.

Printed forms to aid in diagramming the relationship of the track being traced to guide tracks are helpful to the scanner.

There is a serious danger in tracing a track from one pellicle to the next that the observer may inadvertently jump to the track of another particle. This danger is reduced if the stack is well aligned, if the emulsion distortion is small, if the density of other tracks is low, and if careful measurements of angles and the track grain density are made. As an example of a pitfall one can cite the following: on tracing a track from pellicle  $i$  to  $i + 1$ , perhaps only one continuing track may seem possible, but on going from pellicle  $i + 1$  to pellicle  $i$  two are possible. This situation could arise if in pellicle  $i$ , one were actually following a track produced in the emulsion prior to assembling the stack.



# Particle Scattering in Emulsion

In emulsion the centers of the developed grains that define a track do not lie on a straight line. The study of this effect is the subject of this chapter.

The direction of the motion of a charged particle penetrating matter gradually turns and it sometimes changes abruptly. Such "scattering" occurs as the particle passes through intense atomic force fields. Both violent collisions of the moving particle with nuclei that bring about large changes in its direction, and the cumulative effect of many small deflections can be observed and measured. Scattering data, in principle, can provide very complete information about the particle and its interactions. In emulsion the track of each particle, as it slows down and comes to rest, is characteristic of that mass and charge. Its track constitutes the signature of a particle, and it is usually recognizable by an experienced observer.

Much of the scattering is caused by the electric forces between charged particles. The inverse-square force between point charges leads to the Rutherford scattering law. This differential cross section is derivable classically, by the Born approximation, or by an exact quantum mechanical calculation (in the non-relativistic limit).

## 8.1 Scattering of Point Charges by Point Charges

The Rutherford cross section for scattering of a particle of charge  $Z_1e$  through an angle  $\chi_1$ , when its momentum is  $p_1$  and its velocity  $V_1$ , by a heavy point charge  $Z_2e$  is:

$$\frac{1}{4} (Z_2e)^2 \left( \frac{Z_1e}{p_1 V_1} \right)^2 \left[ \csc^4 \frac{\chi_1}{2} \right] \text{ cm}^2/\text{sr} \quad (8.1.1)$$

The first factor is numerical, the second describes the scatterer, the third describes the moving particle, and the fourth contains only the angular distribution with no reference to the medium, the charge, the



mass, or the velocity of the moving particle. This means that if the Rutherford scattering formula were completely valid, the relative probability of various scattering angles would be the same for all particles, in all media at all velocities. Such remarkable behavior would completely determine the measurable scattering of a charged particle track in emulsion. On the other hand, deviations from this predicted behavior are of the highest importance. This is because such deviations reveal details of atomic and nuclear structure and something regarding the strong interactions between elementary particles.

When the mass of the scattered particle is not negligible compared to that of the scattering center, one finds that the Rutherford scattering law is somewhat modified. In the region where classical physics applies, the Rutherford cross section becomes:

$$\frac{d\sigma}{d\Omega} = \frac{Z_1^2 Z_2^2 e^4}{4M^2 V^4} \csc^4 \left( \frac{\chi_1^*}{2} \right) \text{ cm}^2/\text{sr} \quad (8.1.2)$$

In this equation  $\chi_1^*$  is the scattering angle in the center of mass system (CMS) in which the total momentum vanishes. Also  $M = M_1 M_2 / (M_1 + M_2)$ . The quantities  $M_1$ ,  $Z_1 e$  and  $M_2$ ,  $Z_2 e$  are the mass and charge of the colliding particles, 1 and 2, respectively, and  $V$  is the relative velocity of particles 1 and 2.

The Rutherford scattering of a light point charge,  $Z_1 e$ , when viewed in projection is described by the cross section  $\sigma_p(\omega) d\omega$  for scattering through a projected angle  $\omega$  into the angular interval  $d\omega$ :

$$\sigma_p(\omega) d\omega = \frac{2(mc)^2 r_0^2 Z_2^2 Z_1^2}{(p\beta)^2} \frac{1 - (|\omega| - \pi) \cot |\omega|}{\sin^2 \omega} d\omega \quad (8.1.3)$$

The angle  $\omega$  is measured in radians and lies in the interval  $-\pi$  to  $\pi$ . In a material in which there are  $N_i$  atoms of atomic number  $Z_i$  per unit volume, the probability of scattering a particle of momentum  $p$  into the angular interval  $d\omega$  in a horizontal path length  $dx$  is found on replacing  $Z_2^2$  in the above formula by  $\sum_i N_i Z_i^2 / \sum_i N_i$ . The result for standard emulsion is:

$$S(\omega) d\omega dx = \frac{0.7484 Z_1^2}{p^2 \beta^2} \frac{1 - (|\omega| - \pi) \cot |\omega|}{\sin^2 \omega} d\omega dx \quad (8.1.4)$$

where we have also expressed  $p$  in Mev/c.



## 8.2 Electron Screening

The electrons surrounding each atomic nucleus measurably reduce the electric field of the nucleus at points remote from it. Beyond the atomic radius, which is a few times  $a_0 (= \hbar^2/me^2)$ , the electric field goes to zero. This causes the small-angle coulomb scattering of the atom to fall below that given by the Rutherford law.

The problem of nuclear screening has not been treated exactly. For many purposes the first Born approximation with a statistical atom model evaluates the screening correction to the scattering of fast particles with sufficient accuracy. The Born approximation solution of Eq. (8.3.8), below, is valid when the potential energy  $V$  of the particle in the atomic field is small compared with its kinetic energy, or, more exactly, when the amplitude of the scattered wave is small compared to that of the incident.

Let  $\chi^*$  be the angle of deflection of a scattered particle in the CMS. If  $V$  is a function only of  $r$ , the distance between particle and scattering center, the asymptotic solution,  $\psi \xrightarrow{r \rightarrow \infty} \exp(ikr \cos \chi^*) + f(\chi^*)(\exp ikr)/r$  gives the scattered amplitude,  $f(\chi^*)$ , for an unpolarized beam, with  $k = p/\hbar = 1/\lambda$ .

The first Born approximation solution is:

$$f(\chi^*) = \frac{M_1}{\hbar^2 k \sin(\chi^*/2)} \int_0^\infty V(r) \sin[2kr \sin(\chi^*/2)] r dr \quad (8.2.1)$$

The differential scattering cross section  $[d\sigma(\chi^*)]/d\Omega$  is

$$\frac{d\sigma(\chi^*)}{d\Omega} = |f(\chi^*)|^2 \quad (8.2.2)$$

If one writes:

$$f(\chi^*) = \frac{M_1 Z_1 e^2 \lambda^2}{2\hbar^2} \cdot \frac{[Z_2 - F(\chi^*)]}{\sin^2(\chi^*/2)} \quad (8.2.3)$$

then  $F(\chi^*)$  is the "atomic form factor" for an atom which is heavy compared to the scattered particle. Since the atom is normally much heavier than the scattered particle we shall not bother to distinguish  $\chi$  and  $\chi^*$  in the remainder of this section.

Using a crude atom model in which the screening is represented by the factor  $\exp(-r/a_0)$  in the potential,  $(Z_1 Z_2 e^2)/r \exp(-r/a_0)$ , one obtains:

$$f(\chi) = \frac{M_1 Z_1 Z_2 e^2}{\left[ \frac{\hbar^2}{a_0^2} + 4p^2 \sin^2(\chi/2) \right]} \quad (8.2.4)$$



Molière (M 47) has used an approximate expression for the Thomas-Fermi function (F 28) in order to describe better the atomic electron distribution. The region of intermediate scattering angles was bridged smoothly. At large angles Molière scattering is described by the Rutherford law. At small angles Molière's elementary scattering law is equivalent to the Born approximation for the particular atom model chosen.

Since the scattered particle is usually light and of small charge compared to the scattering nucleus we shall now suggest this by a change of notation. We put  $Z_1 = z$  and  $Z_2 = Z$ .

A governing parameter is  $\alpha = (Zz/137\beta)$ . This defines, on the one hand, the regions where the Born approximation is valid ( $\alpha \ll 1$ ), and on the other where Rutherford scattering is asymptotically correct ( $\alpha \gg 1$ ). An angular constant  $\chi_0 = \lambda/a$ , where  $a$  is the Thomas-Fermi unit of length,  $0.466 \times 10^{-8} Z^{-1/3}$  cm, is also introduced. The scattering behavior is represented by the use of a single angular constant  $\chi_a$ . It was evaluated approximately by Molière:

$$\chi_a = \chi_0(1.13 + 3.76\alpha^2)^{1/2} \quad (8.2.5)$$

Then the ratio,  $q(\chi)$ , of the differential scattering cross section to that of Rutherford is taken to be

$$q(\chi) = \chi^4/(\chi^2 + \chi_a^2)^2 \quad (8.2.6)$$

The term containing  $\alpha^2$  in Eq. (8.2.5) is the correction to the Born approximation that is thought to make the Molière theory generally applicable.

At small scattering angles the elementary scattering law of Molière is not precise, but it has been designed to give the mean scattering angle correctly, and for use in calculating multiple scattering it is a very useful approximation.

Recently Nigam, Sundaresau, and Wu (NSW 59) have called into question some of the approximations of Molière's theory, and with a second Born approximation obtain somewhat different formulas. It is stated that Molière's results are correct only to the accuracy of the first Born approximation.

With another approximate form of the Thomas-Fermi potential distribution, Majewski and Tietz (MT 57) give a relatively simple first Born approximation expression for  $f(\chi)$  with  $z = 1$ . It is:

$$f(\chi) = g \left[ \frac{0.255}{(0.246)^2 + p^2} + \frac{0.581}{(0.947)^2 + p^2} + \frac{0.164}{(4.356)^2 + p^2} \right] \quad (8.2.7)$$



Here

$$g = \frac{3^{4/3} h^2 Z^{1/3}}{2^{17/3} \pi^{2/3} e^2 m}, \quad p = \frac{3^{2/3} h c \beta \sin(\chi/2)}{2^{7/3} \pi^{1/3} e^2 Z^{1/3}}$$

Thomas and Umeda (TU 57) recently have calculated numerical values of the atomic scattering factors. They used the more accurate Thomas, Fermi, Dirac statistical atom model for  $Z = 25$  to 80. Their form-factor data have been empirically fitted by the writer. The derived form is:

$$F \approx \frac{Z}{1 + 3.3Z^{1/12}x + 17.3Z^{-1/12}x^2} \quad (8.2.8)$$

where  $x$  is the Bethe variable  $10^{-8}Z^{-1/3} \sin(\chi/2)$ . This is a significant improvement for small deflection angles over that given by the Thomas-Fermi atom model.

The effect of the screening is to replace  $Z$  in the scattering formula by  $Z - F$ . It puts an additional factor,  $q$ , in the Rutherford scattering formula, where

$$q = \left[ 1 - \frac{Z^{1/12}}{17.3(x-a)(x-b)} \right]^2 \quad (8.2.9)$$

The roots  $a$  and  $b$  are the solutions of the quadratic equation

$$1 + 3.3Z^{1/12}y + 17.3Z^{-1/12}y^2 = 0 \quad (8.2.10)$$

The scattering by a neutral atom is then given by the three-term formula:

$$d\sigma(\chi) = \frac{2\pi r_0^2 z^2 Z^{4/3}}{10^{16} \gamma^2 \beta^4} \left[ \frac{dx}{x^3} - \frac{0.1156 Z^{1/12} dx}{x^3(x-a)(x-b)} + \frac{0.00334 Z^{1/6} dx}{x^3(x-a)^2(x-b)^2} \right] \quad (8.2.11)$$

All these calculations treat the electron density as continuous. Since the electrons have finite charges, and are only  $Z$  in number, this approach is inexact. Occasionally one of the electrons may absorb a considerable amount of energy from the moving particle in a close collision. When the energy transferred is large, the electron will be projected into the continuum, and may be observable as a delta ray (Chapter 9). Such an atomic collision is *inelastic*. This means that the sum of the kinetic energy of the incident particle and the scattering atom is not conserved in the collision; work of excitation or ionization has been done. The contribution to the particle scattering arising from such collisions is treated in Section 8.5.

In an important respect the treatment of scattering given thus far is incomplete. The atomic nucleus has been represented merely by a



massive point charge of magnitude  $Ze$ . Such an atomic model will cause the distribution of large scattering angles to be incorrect. The Molière scattering distribution, for example, has a large-angle tail that is too high for weakly interacting particles like muons and electrons, and often too low for strongly interacting particles, although a region of interference between the strong and electromagnetic scattering by the nucleus generally will exist.

### 8.3 Nuclear Scattering

#### 8.3.1 Nuclear Size Effects

Atomic nuclei are not point charges. Indeed, their structure and whatever structure of the elementary particles can be observed in nuclear reactions largely constitute the subject matter for nuclear and subnuclear physics.

The finite sizes of the scattering centers cause deviations from Rutherford scattering.

The theory that is used to discuss nuclear scattering depends on the particle radian length,  $\lambda = \hbar/p$ . The position of a particle is well defined if  $\lambda$  is small. The impact parameter is a meaningful concept if it remains large compared to  $\lambda$ . If the impact parameter is not greater than the nuclear radius, the potential is no longer purely Coulombic and gives rise to deviations from the Rutherford law. For a beam of a given energy, this effect is most conspicuous at large angles of deflection. The range of nuclear forces is about equal to the pion Compton-length,  $\lambda_\pi \equiv \hbar/m_\pi c = 1.41$  fermi (1 fermi =  $10^{-13}$  cm). The effective radius of a nucleus of mass number  $A$  for fast, strongly interacting particles is about  $\lambda_\pi A^{1/3}$ . When two complex nuclei, 1 and 2, collide at high energy, the inelastic collision cross section is about  $\pi \lambda_\pi^2 (A_1^{1/3} + A_2^{1/3})^2$ . This has been tested for alpha particles in emulsion (W 56.1). It was found that  $\lambda_\pi A^{1/3}$  slightly overestimates the nuclear radius effective for disintegration collisions.

Scattering, as well as collisions causing disintegration, are frequently observed when the tracks of complex nuclei in emulsion are studied. Interactions with both the light and heavy nuclei are identifiable, and rather complete classification of the processes taking place is possible. The Rutherford scattering of ions with energies up to 10 Mev per nucleon can be treated completely by classical mechanics, thus simplifying the analysis. In virtue of its large mass, the radian length,  $\lambda$ , of a 100 Mev oxygen ion, for example, is about  $10^{-14}$  cm, and the relativistic factor  $\gamma = (1 - \beta^2)^{-1/2}$  remains within 1% of unity.

Suppose a nucleus of mass  $M_1$  and charge  $Z_1 e$  is deflected through



an angle  $\chi_1^*$  in the CMS by the Coulomb field of a nucleus of charge  $Z_2e$  and mass  $M_2$  (see Section 8.1). The *impact parameter*,  $b$ , is defined to be the perpendicular distance from nucleus 2 to the asymptote of the trajectory of particle 1 in the laboratory system, LS, or the distance between the parallel asymptotes of 1 and 2 in the CMS. The distance of closest approach,  $b_0$ , is the smallest distance between the centers that is attained in a collision. Now  $M = (M_1M_2)/(M_1 + M_2)$ , is the reduced mass. Then

$$b = \frac{Z_1Z_2e^2}{MV^2} \cot(\chi_1^*/2) \quad (8.3.1)$$

where  $\chi_1^*$  is the angle of deflection of particle 1 in the CMS, and  $V$  is its velocity in the laboratory system before scattering.

In the laboratory the angular distribution is not that given by Eq. (8.1.1). The angle,  $\chi_1$ , in the laboratory is, however, rather simply related to that in the center of mass:

$$\tan \chi_1 = \frac{\sin \chi_1^*}{\cos \chi_1^* + M_1/M_2} \quad (8.3.2)$$

Then

$$\chi_1 = \arctan \frac{2(q^2 - 1)^{1/2}}{\left(1 + \frac{M_1}{M_2}\right)q^2 - 2} \quad (8.3.3)$$

where  $q = \csc(\chi_1^*/2)$ . The quantity  $q$  is best related to the observed scattering angle  $\chi_1$  by a set of curves corresponding to the appropriate ratios  $M_1/M_2$ .

In the laboratory an elastically scattered nucleus loses energy,  $\Delta T$ , given by

$$\Delta T = \frac{4M^2T_1}{M_1M_2q^2} \quad (8.3.4)$$

where  $T_1$  is the kinetic energy before scattering. The scatterer gains the energy,  $\Delta T$ . When this is big enough to measure it can be used to evaluate  $M_2$ .

A condition for the scattering to remain of the Rutherford type is that the particle radii do not overlap at the distance of nearest approach. The effective radius of a nucleus, as stated above, is about  $\lambda_\pi A^{1/3}$ . The minimum distance,  $b_0$ , for Rutherford scattering, accordingly, will be about  $\lambda_\pi(M_1^{1/3} + M_2^{1/3})$ , where  $M_1$  and  $M_2$  are expressed in units of the



proton mass. By solving the orbit equations one can find the distance of nearest approach,  $b_0$ . It is

$$b_0 = \frac{Z_1 Z_2 e^2}{MV^2} (1 + q) \quad (8.3.5)$$

Therefore, in a diagram in which the kinetic energy  $T_1$  of  $M_1$  is plotted against  $q$ , a straight line is obtained for a given value of  $M_2$ . There is a line corresponding to each scattering element in emulsion. The intercept on the kinetic energy axis and the slope are each equal to  $(M_1 Z_1 Z_2 e^2)/(2Mb_0)$ . Values of  $b_0$  are chosen equal to the sum of the radii of beam nucleus and target. A  $(q, T_1)$  point plotted on such a diagram corresponds to a nuclear interaction if it lies above the line and to Rutherford scattering if it lies below the line.

Because it is most directly related to sensory experience, we have carried as far as practicable the description of scattering that is derived from classical mechanics. While it has a large domain of validity for Coulomb scattering, this approach nevertheless is completely inadequate to describe *nuclear* scattering or the Coulomb scattering of identical systems.

In textbooks on quantum mechanics, nuclear scattering usually is treated by first expressing the energy of particle plus scatterer as a Hamiltonian. The Hamiltonian, in operator form, yields the wave equation. The nature of the scattering will depend on the potential terms describing the interaction of the beam and scatterer. One can calculate the scattering of any kind of particle if the interaction is correctly formulated, and if the resultant wave equation can be solved. Sometimes more than one "scattering channel" may be present, corresponding to various energetically possible alternative things that could happen. These might be elastic scattering, charge-exchange scattering, annihilation, etc.

Considered thus generally, nuclear reactions and elementary particle reactions are included in this scattering formalism. For a given composite system of  $n$  channels and total energy  $E$ , a matrix, e.g., the  $S$ -matrix of Heisenberg (H 43), gives the probability for scattering into each channel. It would be going too far afield, however, to elaborate in this book the important conservation and reciprocity theorems (BW 52) for nuclear reactions that are stated in terms of such matrix elements.

In modern theory all "forces" are brought about by absorptions and emissions of particles. Such exchanges are believed necessary for a scattering event to take place. The range of the force varies inversely with the mass of the object exchanged. Thus, for example, the Coulomb



force arises from the exchange of photons, and the long range nucleon-nucleon force from the exchange of a single pion. Close collisions probably involve multiparticle exchanges and exchanges of  $K$  meson pairs.

In the past it was usually possible to study the scattering only if the target was relatively stable. Chew and Low (CL 59), however, showed how to analyze the process so as to observe the scattering by unstable targets, particularly by pions.

The scattering of electrons by any charged particle, stable or unstable, in principle can be studied merely by causing the particle to traverse emulsion with a high velocity. In the particle rest frame, the electrons of the emulsion constitute a beam which is scattered by the particle. When viewed in the laboratory frame the interactions are made evident by tracks of electrons which are projected from the path of the particle. Let  $\theta$  be the angle of the electron motion to the primary direction and  $w$  the energy transferred to the electron. Then  $\sec^2\theta = \beta_0^2(1 + 2m/w)$  where  $m$  is the electron mass and  $\beta_0$  is the velocity of the center of mass system. Often the energy is so high that  $\beta_0$  can be set equal to unity. Then if  $\theta$  also is small  $\theta^2 \approx 2m/w$ .

One of the most important problems of modern physics is posed by the strong interactions existing between the various baryons, between mesons and baryons, and between mesons. The large binding energies of nuclei first revealed the existence of the strong interactions. In emulsion, as in all matter, the strong interactions of mesons and baryons in their nuclear scattering behavior is conspicuous. On the other hand, charged leptons display only electromagnetic and weak interactions, while neutral leptons (neutrinos) have only weak interactions. Photons are limited to electromagnetic interactions. Only electromagnetic and strong interactions bring about the scattering of particles in matter. The particles that do not experience strong interactions are scattered only by the distributions of electric charges and currents in the scattering center.

For the treatment of strong interactions a more modern approach than the Hamiltonian method has been found in the powerful dispersion theory which formulates the scattering problem more directly in terms of measurable quantities. It provides for Lorentz invariance; it permits no instantaneous action at a distance, as do some potential scattering formulations; and it is a unitary theory which encounters no divergences. Substantial progress in developing quantitative strong interaction theory may come from this approach (DO 60).

Most of modern strong-interaction theory remains outside the scope of this book, however. For this chapter it is desirable merely to make an elementary summary of the concepts and notation of potential scattering, and to treat somewhat descriptively the scattering and



interaction processes that are observed in emulsion. Aside from the study of bound states of particle systems, the scattering-reaction processes are the chief strong-interaction phenomena accessible to experiment.

### 8.3.2 Analysis of Scattering

The elementary theory of potential scattering is reviewed as follows:

The total energy in the CMS (particle plus scatterer), is put in the Hamiltonian form:

$$H(p, q) = E \quad (8.3.6)$$

The incident beam at infinity is described by a plane wave. The wave has amplitude  $\Psi$ . One can write

$$H(p, q) \Psi = E \Psi \quad (8.3.7)$$

Then, by the inductive logic of Schrödinger (S 26)  $p$  is replaced by  $-i\hbar\nabla$  and  $E$  by  $i\hbar(\partial/\partial t)$ .

On factoring out the time-dependence there remains the nonrelativistic wave equation in the CMS.

$$\left[ \nabla^2 + \frac{2M}{\hbar^2} (E - V) \right] \psi = 0 \quad (8.3.8)$$

Here  $M = M_1 M_2 / (M_1 + M_2)$  and  $E - V$  is the kinetic energy.

General methods for the approximate calculation of the scattering distribution valid under various conditions are given in all works on quantum mechanics. Probably the most important is the method of the Born approximation, used elsewhere in this book, in which the whole potential energy term is regarded as a perturbation of a plane wave solution. More generally, the perturbation method is used when the wave equation with a particular potential cannot be solved, but it can be with a slightly different one. The difference between the two potentials is treated as a small perturbation. The solution of the perturbed system can be written as a linear combination of the characteristic solutions of the unperturbed equation because they form a complete set. Then by substitution in the original equation, the coefficients of this expansion are found in terms of the matrix elements of the perturbation. In other circumstances the WKB solution or a variational method may be useful.

The partial wave solution of the wave equation, which we owe to Lord



Rayleigh, may be sought when approximate methods do not serve. The form of solution for a central force is (FH 27):

$$\psi = \sum_{l=0}^{\infty} R_l(r) P_l(\cos \chi) \quad (8.3.9)$$

Then (see Section 8.2)  $f(\chi)$  is

$$f(\chi) = k^{-1} \sum_{l=0}^{\infty} (2l+1) e^{i\delta_l} \sin \delta_l P_l(\cos \chi) \quad (8.3.10)$$

while  $\delta_l$  is found from the asymptotic value of  $R_l(r)$ . It is:

$$R_l = r^{-1} U_l \rightarrow A_l (kr)^{-1} \sin(kr - \frac{\pi}{2} l - \delta_l) \quad (8.3.11)$$

The form of  $U_l$  is found from the solution of the radial wave equation:

$$\frac{d^2 U_l}{dr^2} + \left[ k^2 - \frac{2MV}{\hbar^2} - \frac{l(l+1)}{r^2} \right] U_l = 0 \quad (8.3.12)$$

The solution with  $r \rightarrow \infty$  gives the phase shift  $\delta_l$ . From the resulting value of  $f(\chi)$  the differential scattering cross section  $[d\sigma(\chi)]/(d\Omega)$  is found.

$$\frac{d\sigma(\chi)}{d\Omega} = |f(\chi)|^2 = \frac{1}{k^2} \left| \sum_{l=0}^{\infty} (2l+1) e^{i\delta_l} \sin \delta_l P_l \right|^2 \quad (8.3.13)$$

The total cross section for scattering is

$$\sigma = \frac{4\pi}{k^2} \sum_{l=0}^{\infty} (2l+1) \sin^2 \delta_l \quad (8.3.14)$$

When the scattered particle is charged, part of the phase shift  $\delta_l$  will be caused by the Coulomb field of the scattering center.

If the velocity is so low that only the  $s$ -wave phase shift  $\delta_0$  determines the cross section, the "effective range theory" introduces a great simplicity. The phase shift and momentum then are related by the equation

$$k \cot \delta_0 \approx (-1/a) + (1/2) r_0 k^2$$

where  $a$ , the scattering length, is defined by

$$1/a = -\lim_{k \rightarrow 0} (k \cot \delta_0) \quad (\text{a constant})$$



and  $r_0$ , the effective range, is given by

$$r_0 = 2 \int_0^\infty (U_0^2 - V_0^2) dr$$

which is also a constant when  $U_0$  and  $V_0$  are the respective zero-energy wave functions that have the same asymptotic behavior when the scattering force is turned on and off. The form of the function gives a straight line when  $k \cot \delta_0$  is plotted against  $k^2$ , and the scattering length and effective range are found from the intercept and slope.

In the case where the  $s$ -wave is not present as in pion-nucleon scattering near the  $3/2$ ,  $3/2$  resonance (see below), a similar effective range analysis can be made of the pion-nucleon interaction (CL 56).

The effect of the multiple scattering of a particle within a nucleus is as if the particle wave were refracted by the nuclear matter. The effect of the medium is to change the propagation constant, which is  $k$  in free space, to  $k' = [k^2 + 4\pi\rho f(0)]^{1/2}$ , where  $f(0)$  is the forward scattering amplitude of the wave, and  $\rho$  is the density of scattering centers. Nucleon correlation effects are to be included in  $\rho$ .

The effective index of refraction,  $\mu$ , is given by  $\mu^2 = 1 + 4\pi\rho\lambda^2 f(0)$ , where  $\lambda = 1/k$  is the radian length of the wave. It is also possible to describe the scattering by assuming that within the nucleus, the particle experiences a potential  $V = -(2\pi\hbar^2/M)\rho f(0)$ , where  $M$  is the reduced mass of the particle-nucleon system. Because the particle experiences inelastic collisions,  $V$  is complex and is written  $V = -(V_0 + iW_0)$ . The model of nuclear scattering based on these premises is called the optical model.

The relativistic Schrödinger equation, the Klein-Gordon equation, is often needed in scattering calculations. It can be obtained from Eq. (8.3.7). It requires only that in the wave mechanical formula,  $\lambda = \hbar/p$ , the relativistic momentum be used. The numerical form is:  $k^{-1} = \lambda = 197.32/p$  fermi (1 fermi is  $10^{-13}\text{cm}$ ), when  $p$  is in Mev/c. Then the Schrödinger Equation can be written

$$\nabla^2\psi + k^2\psi = 0 \quad (8.3.15)$$

where  $k\hbar$  is the *local* value of the momentum. The nonrelativistic expression for the momentum leads to Eq. (8.3.8). To make it relativistic one merely puts  $(E - V)^2 - M_1^2C^4$  for  $k^2\hbar^2$ . The total energy  $E$  includes the rest energy  $M_1C^2$  of the incident particle. This relativistic Schrödinger equation is adequate for scattering that requires only a simple scalar wave function for its description.

The physical problem often is about as follows: the scattering can be



observed, but the potential,  $V$ , is unknown. It is hoped that from the observed scattering that the law of force may be deduced. This can be attempted by assuming a plausible model for the scatterer in which are included adjustable parameters. For each set of parameters a solution is found and compared with the experimental data. A set of parameters for each model can be determined in this way that most nearly describes the observed scattering.

For an example of this type of analysis we cite the work of Melkanoff *et al.* (MPST 59), who made an optical model analysis of the scattering of 125 Mev  $K^+$  mesons in emulsion.

Assuming  $T \gg V$ , they reduced Eq. (8.3.15) to

$$\nabla^2 \psi + k_0^2 \left[ 1 + \frac{V_T}{T} \left( \frac{1 + \alpha}{1 + \alpha/2} \right) \right] \psi = 0 \quad (8.3.16)$$

Then the equation for  $U_l$  is:

$$\frac{d^2 U_l}{dr^2} + k_0^2 \left[ 1 - \frac{V_T}{T} \left( \frac{1 + \alpha}{1 + \alpha/2} \right) - \frac{l(l+1)}{k_0^2 r^2} \right] U_l = 0 \quad (8.3.17)$$

In these equations  $T = E - M_1 C^2$ ,  $\alpha = T/(M_1 C^2)$ , and  $k_0^2 = [(2M_1 T)/\hbar^2] [1 + (1/2)\alpha]$ . The mass  $M_1$  of the  $K$  meson was considered small compared to the nuclear mass but a correction for this approximation was later applied. Relativistic effects were merely first-order corrections to the nonrelativistic theory in virtue of the approximations made.

The form of the potential  $V_T$  was derived from the diffuse-surface optical model of a nucleus. It was made up of the sum of two parts, a nuclear part  $V_N$ , and a Coulomb part  $V_C$ .

$$V_N = (V + iW)/\{1 + \exp [(r - R)/a]\} \quad (8.3.18a)$$

and

$$\begin{aligned} V_C &= (Ze^2/2R) (3 - r^2/R^2) \quad \text{for } r \leq R \\ &= Ze^2/r \quad \text{for } r \geq R \end{aligned} \quad (8.3.18b)$$

The effective nuclear radius  $R$  was assumed to have the form  $R = R_0 A^{1/3}$  for all the emulsion nuclei (except hydrogen). The four parameters  $V$ ,  $W$ ,  $R_0$ , and  $a$  were assumed to have the same values independent of atomic number. The parameter  $W$ , which causes the "index of refraction" of the nucleus to be complex, was adjusted to give the observed reaction cross section. Using computing machinery, Eq. (8.3.17) was solved for each value of  $l$  contributing to the non-Coulombic scattering.



For large values of  $l$  the solutions joined those for a Coulomb field. In the region where both nuclear scattering and Coulomb scattering are present, constructive interference was found; thus implying that the nuclear potential is repulsive. For two values of  $R_0$ , and  $a = 0.57 \times 10^{-13}$  cm, the following values of  $V$  and  $W$  best fit the data:

$$R_0 = 1.07 \times 10^{-13} \text{ cm}, \quad V = 23 \pm 4 \text{ Mev}, \quad W = -9.7 \pm 1.3 \text{ Mev}$$

$$R_0 = 1.20 \times 10^{-13} \text{ cm}, \quad V = 14 \pm 3 \text{ Mev}, \quad W = -6.4 \pm 0.9 \text{ Mev}$$

Most scattering by the complex nuclei of emulsion at present is best treated by the optical model.

An important fraction of the scattering centers in emulsion are free protons. The elastic scattering of protons by protons in emulsion has been the subject of many studies. For example Duke *et al.* (D-M 57) observed the scattering of 925 Mev protons. Some of the general problems in such an experiment are the following: (a) a collimated proton beam of the correct intensity is required. This should be perhaps  $10^5$  protons per square centimeter. The precise control of the intensity and the production of a proton beam that does not contain degraded particles are matters of experimental skill. (b) The scanning must be free of bias. The particular two-prong stars studied in this experiment were not difficult to see, but at the minimum of ionization this would become a serious problem. Certain dip angles of the products tend to cause them to be missed and tests for such biases were made by Duke *et al.* They found a severe loss when the dip angles were large and the scattering angles small.\* (c) Not all the apparent scatters are true proton-proton elastic events. Measurements must be made to test for conservation of energy and momentum in the collision. The simplest is to check for coplanarity. The angles also are simply related to each other. By analyzing the statistical error of measurement the collisions can be classified into a group which is probably elastic and another group of inelastic plus

\* In similar work, the writer has found that exposure of the emulsion with the beam entering the pellicle perpendicular to its surface has some great advantages when the beam energy is high. One scans such plates by varying the fine-focus control while watching one track or a small bundle of tracks. Where a proton-proton collision occurs, the track suddenly splits into two. The space angle with respect to the original direction of each is easily measured with this geometry. The relation connecting these angles  $\theta$  and  $\phi$ , is  $\tan \theta \tan \phi = 2/(\gamma + 1)$  where  $\gamma = (1 - \beta^2)^{-1/2}$  and  $\beta c$  is the velocity of the incident proton.

Since the multiple scattering is small when the energy is high, this method of scanning detects scattering of all sorts with good efficiency. The various tracks appear in the focal plane as dots that do not change their relative positions on varying the focusing adjustment unless one of the particles scatters (G 55).



quasi-elastic events. In inelastic scattering, mesons are produced, and in quasi-elastic scattering the collision simulates elastic scattering, but is with a bound proton in a complex nucleus. An inelastic process that may simulate proton-proton scattering is one in which two prongs, one or both of which are charged mesons, emerge from the collision. In other cases only neutral mesons are produced. (d) To obtain absolute cross sections, the hydrogen content of the emulsion must be known, the true track length scanned must be calculated, and the scanning efficiency correctly evaluated (see Chapters 3 and 7). (e) To obtain differential cross sections, angles must be measured allowing for the shrinkage factor and making the relativistic transformations to the CM system (see Volume II).

High-energy elastic proton-proton scattering with large angular momentum has a Coulomb component corresponding to exchange of a photon of zero mass. This has a scattering amplitude containing the factor  $(1 - \cos \theta)^{-1}$ . Next in order of decreasing range is the one-pion exchange. This contains the angular factor  $[1 + (\mu^2/2p^2) - \cos \theta]^{-1}$ , where  $\mu$  is the pion mass and  $p$  is the momentum. Small angular momenta correspond to close collisions, the exchange of more massive objects, and multiple exchanges. At present their analysis cannot be approached from as fundamental a point of view as the peripheral collisions.

Duke *et al.* found a total elastic cross section of  $13 \pm 3 \times 10^{-27} \text{ cm}^2$ . The scattering was strongly peaked at small angles. Giles (G 55) found the elastic proton-proton cross section at 5.7 Bev to be  $13 \pm 6 \times 10^{-27} \text{ cm}^2$  in a very early emulsion observation.

An antiproton-proton elastic scattering cross section was measured in emulsion by Ekspong and Ronne (ER 59). They found  $77 \pm 17 \times 10^{-27} \text{ cm}^2$  for it. In the interval 30-250 Mev, the free path for annihilation is given as  $20.8 \pm 1.6 \text{ cm}$ , and the interaction free path as  $18.3 \pm 1.3 \text{ cm}$ . The inelastic scattering cross section from the complex nuclei is only  $(42 \pm 11) \times 10^{-27} \text{ cm}^2$  per emulsion nucleus, while the elastic scattering is consistent with a combination of Rutherford and diffraction scattering from a completely absorbing nucleus.

The low-energy pion-nucleon scattering is best discussed with reference to the elegant angular momentum—isospin combinational analysis (SBD 55). The pion exists in three charge states, so the total isospin is unity, with projections of 1, 0, -1. Its spin is zero. The nucleon isospin is  $1/2$  and its spin is also  $1/2$ . In combination, the isospin of the pion-nucleon system therefore has two possible values:  $I = 1/2$  and  $I = 3/2$ . To the nucleon spin, the orbital angular momentum is to be added, the states being  $S_{1/2}$ ,  $P_{1/2}$ ,  $P_{3/2}$ , etc. States of orbital angular momentum  $l$  will be revealed in the scattering cross section



by the presence in it of the  $2l - 1$  and  $2l$  powers of  $\cos \theta$ . If only  $s$  and  $p$  scattering occur, differential cross section for each scattering process can be written

$$\sigma = a + b \cos \theta + c \cos^2 \theta \text{ cm}^2/\text{sr} \quad (8.3.19)$$

The interactions that have been studied are:

$$\pi^+ + p \rightarrow \pi^+ + p \quad (8.3.20a)$$

$$\pi^- + p \rightarrow \pi^- + p \quad (8.3.20b)$$

$$\pi^- + p \rightarrow \pi^0 + n \quad (8.3.20c)$$

Corresponding to the possible states of angular momentum and isospin, six phase shifts  $\delta_3(S_{1/2}, I_{3/2})$ ,  $\delta_{31}(p_{1/2}, I_{3/2})$ ,  $\delta_{33}(p_{3/2}, I_{3/2})$ ,  $\delta_1(S_{1/2}, I_{1/2})$ ,  $\delta_{11}(p_{1/2}, I_{1/2})$ , and  $\delta_{13}(p_{3/2}, I_{1/2})$  are sufficient at a given energy to give the nine coefficients of the angular distributions in Eq. (8.3.20). Conversely, the nine coefficients in principle overdetermine the phase shifts. There of course remains some ambiguity and error in the phase shifts because of the limited accuracy of the experimental data. In the first solutions found by Glicksman (G 54.2) it was necessary to take only the phase shifts  $\delta_3$ ,  $\delta_1$ , and  $\delta_{33}$  different from zero. At low velocities the  $\delta_3$  and  $\delta_1$  phase shifts depend linearly on the momentum in the CMS. Remarkable features of the pion-nucleon scattering are the spectacular resonances in the cross sections. The phase shift  $\delta_{33}$  passes through  $90^\circ$  at an energy of about 194 Mev. This greatly increases both the  $\pi^+p$  and  $\pi^-p$  cross sections, but the  $\pi^+p$ , being a pure state, is affected more. At low velocities  $\delta_{33}$  seems to vary with the cube of the momentum. In this region the phase shifts are expected to vary with  $p^{2l+1}$ . At high energies further resonances appear, and the simple theory no longer applies. The possibility of meson production and higher angular momenta complicate the interpretation. *D*-state scattering has been observed at high meson energies.

The amplitudes giving the total cross sections of Eqs. (8.3.20a, b, and c) can be expressed in terms of two scattering amplitudes  $a(3/2)$  and  $a(1/2)$ , corresponding to the isospin states  $3/2$  and  $1/2$  as follows:

$$\pi^+ + p \rightarrow \pi^+ + p \quad a^{++} = a(3/2) \quad (8.3.21a)$$

$$\pi^- + p \rightarrow \pi^- + p \quad a^{--} = 1/3[2a(1/2) + a(3/2)] \quad (8.3.21b)$$

$$\pi^- + p \rightarrow \pi^0 + n \quad a^{-0} = \frac{(2)^{1/2}}{3} [-a(1/2) + a(3/2)] \quad (8.3.21c)$$



The unobserved scattering of  $\pi^0$  mesons by hydrogen is also predicted to be:

$$\pi^0 + p \rightarrow \pi^0 + p \quad a^{00} = 1/3[a(1/2) + 2a(3/2)] \quad (8.3.21d)$$

In addition, the reactions that are mirror images of Eq. (8.3.21) are predicted to be identical superpositions of scattering amplitudes.

In order to determine the sign of the interaction potential between the proton and positive pion in the  $(3/2, 3/2)$  resonance region, the scattering at small angles can be examined to determine whether the Coulomb scattering contribution is constructive or destructive.

Good angular resolution is attainable when emulsion is used as the detector-analyzer of  $\pi$ - $p$  scattering. Orear (0 54), with a  $\pi^+$  beam of average energy 113 Mev, found 420  $\pi^+$ - $p$  scattering events in emulsion. By making an analysis of the angular distribution, he was able to show that the interference between the Coulomb scattering and the  $(3/2, 3/2)$  resonance scattering was destructive, and therefore that the  $p_{3/2}$  interaction was attractive. The signs of all the phase shifts then follow.

Below 100 Mev three phase shifts are sufficient to describe the scattering, which can be given analytically as follows:

$$\begin{aligned} \delta_1 &= 0.17\eta \\ \delta_3 &= -0.11\eta \\ \delta_{33} &= 0.235\eta^3 \end{aligned} \quad (8.3.22)$$

where  $\eta = \beta/(1 - \beta^2)^{1/2}$ ,  $\beta c$  being the velocity of the pion.

A simple type of scattering that does not depend on the details of the nuclear potential occurs when the beam is strongly absorbed by nuclei and is of such high momentum that the particle wavelength is small compared to the nuclear radius,  $R$ . The type of scattering that occurs then, in analogy to optics, is called "diffraction" scattering. In the ideal limit of very strong absorption, the nucleus behaves like an opaque disk. The wavelength being short, the nucleus removes from the beam the particles in an area  $\pi R^2$  of the wave front. The absorption cross section is, therefore,  $\pi R^2$ . The wave is also diffracted, and bends into the region behind the nucleus. The differential cross section of this "shadow scattering" is (BP 37):

$$\frac{d\sigma_{sc}(\chi)}{d\Omega} = R^2 \left[ \frac{J_1(kR\chi)}{\chi} \right] \quad (8.3.23)$$

Here the beam particle is considered light compared to the nucleus,  $\chi$  is assumed small,  $k = p/\hbar$ , and  $J_1$  is the usual Bessel function. The scattering cross section is  $\pi R^2$ , so the total cross section is  $2\pi R^2$ .



A single scattering event along the path of a particle may be sufficient to identify the particle making a track. Suppose a mixed beam of pions and muons traverse emulsion after being analyzed by a magnet. Because it is not affected by nuclear forces, the cross section for large single scattering of a muon of this momentum becomes very low for angles larger than  $\approx A^{2/3}/(p\beta)$  radians, where  $A$  is the atomic mass number. Consequently, a particle of say 350 Mev/c that is deflected more than about  $4^\circ$  in emulsion can be considered to be a pion with a high probability.

The only large angle scattering sustained by a muon of this momentum is the incoherent muon-nucleon scattering which is attributed largely to the magnetic moment of the nucleon.

In emulsion the scattering of identical particles ( $e^- - e^-$ , proton-proton,  $C^{12} - C^{12}$ , etc.) is not infrequently observed. In such collisions the identity of the particles requires that in the CMS. the cross section for angle  $\chi^*$  is the same as for angle  $\pi - \chi^*$ .

Furthermore at angle  $\chi^*$  the amplitude is  $f(\chi^*) + f(\pi - \chi^*)$ , because for each beam particle at  $\pi - \chi^*$ , a scattering particle will be projected at angle  $\chi^*$ .

When the particles have Fermi statistics, only wave functions that are antisymmetric with respect to the exchange of the particles contribute to the scattering cross section. When, like  $C^{12}$ -nuclei, they obey Bose-Einstein statistics only symmetrical states contribute.

When the beam energy is such that the total energy of the target plus beam particle is near one of the "stationary states" of the compound system, a resonance accompanied by an anomaly in the scattering occurs.

A remarkable "molecular" state of two  $C^{12}$ -nuclei was found by Almqvist *et al.* (ABK 60). They studied the scattering of  $C^{12}$  by  $C^{12}$  in the energy range 9-29 Mev. Broad resonances with a spacing of approximately 300 Kev were found. A compound  $Mg^{24}$ -system with an excitation energy of approximately 20 Mev would have sharper resonances and a much closer spacing. The high energy required for the transfer of a nucleon from one carbon nucleus to the other can account for the retention of the identities of the two carbon nuclei in the "molecular" state. In this state, the spin is measured in the hundreds of units of  $\hbar$ . Although this scattering process has not been reported in emulsion, the presence of a large amount of carbon in emulsion probably would make its study feasible. Details not obtainable from the counter data should be visible. Emulsion also could be used profitably with an external carbon target and magnetic analysis of the products of the scattering and reaction.



### 8.3.3 Scattering of Polarized Particles

The amplitude,  $f(\chi)$ , has thus far been taken independent of the angle  $\phi$  around the beam axis. It is true that, unless the beam is polarized, the scattering depends just on  $\chi$ . In recent years, however, polarization of particles with spin has been observed and polarized beams have been employed, so that in some experiments the angle  $\phi$  is an important variable. A more complete understanding of the forces producing scattering is obtained from a scattering amplitude

$$f(\chi, \phi) = g(\chi) + h(\chi) \boldsymbol{\sigma} \cdot \mathbf{l}$$

Here  $\boldsymbol{\sigma}$  is the spin matrix and  $\mathbf{l}$  is the unit vector perpendicular to the plane of scattering. The polarization is produced by the term  $h(\chi)\boldsymbol{\sigma} \cdot \mathbf{l}$ . Were there only central forces a dependence of the scattering on the angle  $\phi$  would not be possible. The large polarizations observed in scattering as well as other evidence, such as the electric quadrupole moment of the deuteron and the nuclear shell effects, show that noncentral forces are present in nucleon-nucleon and nucleon-nucleus scattering.

To a limited extent emulsion can be used as an analyzer of polarized beams. When an unpolarized beam of particles traverses emulsion, the scattering populates all angles around the beam direction equally. A longitudinal polarization of the beam produces the same behavior; but, in general, a transverse polarization will influence this angular distribution. While an asymmetry in the  $\phi$  distribution is sufficient to establish a polarization, symmetry in the distribution does not establish lack of polarization. Observations made by Maglić and Feld (MF 57), Grigoriev, (G 55.1), and Friedman (F 56) show that an asymmetry is present for protons, but depends very much on the angle of observation and the particle energy.

Grigoriev (G 55.1) apparently was the first to find polarization effects in emulsion. He observed asymmetry in the emission of fast prongs from stars produced by 750 Mev polarized protons and neutrons. Subsequent experiments were made by Friedman (F 56) at the instigation of Enrico Fermi, who suggested the use of emulsion to study the polarization process. In particular it was desired to determine whether the polarization was produced in elastic or quasi-elastic scattering process. The inelastic events are detectable in emulsion, and even the approximate excitation energy imparted to the nucleus can be determined. By along-the-track scanning, interactions can be found. Some are elastic. Others are inelastic but are only detectable by the change of grain density of the track at the point where it is deflected and loses energy. A conspicuous



group of inelastic events consisted of those in which charged evaporation prongs emerged from the excited nucleus.

The polarization resulting from  $3^\circ$ - $15^\circ$  elastic scattering of 310 Mev protons was found to be  $0.44 \pm 0.13$ . The polarization produced by inelastic scattering was also studied. It was higher when the angle and energy conditions for quasi-elastic scattering were required. It fell when there was a large energy transfer to the nucleus.

For analysis of polarized particle beams Maglić and Feld pointed out that emulsion in the dual role of scatterer and detector has important advantages; namely a high angular resolution and a large effective target thickness. It also can usually be placed very close to the source, thus making it possible to analyze simultaneously all the particles emitted in a large solid angle. They and a number of collaborators (FM 58, PMF 59, MF 59, FMD 59, MFD 61) have studied the asymmetry of the scattering of protons in emulsion and observed a gross asymmetry of the scattered tracks from a well-collimated polarized beam. Thus both multiple and single scattering effects were included, and individual tracks were not followed. By this technique they report that the scanning time is greatly reduced. For protons of energy of about 135 Mev scattered through angles of  $5^\circ$  to  $12^\circ$  they found that the degree of polarization produced in emulsion was  $60 \pm 6\%$ . When only angles need be measured, a mechanical scanning device can carry out the work very rapidly. They mention that polarized protons can be slowed down by ionization in emulsion to  $\approx 150$  Mev without appreciable depolarization.

Below about 130 Mev the polarization produced by scattering on most nuclei falls rapidly so that the method cannot be used in this region. One should also be aware that the polarization is low in some angular intervals and may reverse its sign. The angles at which these effects occur vary with particle energy. Since in addition a large component of isotropic flux tends to obscure the effect, polarization measurements in emulsion are difficult. The subtraction of the background can lead to a spurious angular asymmetry if the beam is asymmetric. Maglić and Feld (MF 59) recommend along-the-track scanning when the beam is not well collimated and when background tracks are present.

For determining the polarization of 150 Mev protons in emulsion, Sternheimer (S 58.4) carried out an optical model analysis in which he simulated silver bromide by the element niobium ( $Z = 41$ ). The polarization, which arises because of a spin-orbit coupling term in the Hamiltonian, was studied as a function of the imaginary part (the other parts of the scattering potentials having been established in previous work) of a complex scalar function  $U = U_r + iU_i$  which multiplied  $\sigma \cdot \mathbf{L}$ , where  $\mathbf{L}$  is the orbital angular momentum and  $\sigma$  is twice the spin